

**Title: Review study of
the skeleton of
elasmobranchs: a
pathological case of the
butterfly ray (*Gymnura
altavela*) cartilage.**

Student:

Haniel Iribarren Docampo

Tutor:

Ayoze Castro Alonso

Collaborative Tutor:

María José Caballero
Cansino.

Academic course:

2024-2025





INDEX

| | |
|---|----|
| 1. ABSTRACT..... | 1 |
| 2. INTRODUCTION | |
| 2.2.History and taxonomy..... | 1 |
| 2.3.Description of the ecology of the family Gymnuridae..... | 6 |
| 2.4.Ecobiological description of <i>Gymnura altavela</i> | 7 |
| 2.5.Current situation of the butterfly ray in the world..... | 8 |
| 2.6.Importance of the species in the Canary Islands..... | 9 |
| 2.7.Anatomy and histology of the skeleton of batoid fishes..... | 10 |
| 3. OBJECTIVE | |
| 3.2.Description of the normal osteology of the <i>Gymnura altavela</i> skeleton..... | 15 |
| 3.3.Description of the histopathology due to trauma in a <i>Gymnura altavela</i> | 15 |
| 4. MATERIAL AND METHODS | |
| 4.2.Origins of the Specimens..... | 16 |
| 4.3.Macroscopic assessment..... | 18 |
| 4.3.1. Imaging test performed..... | 18 |
| 4.3.2. Necropsy procedure..... | 18 |
| 4.4.Microscopical Assessment..... | 19 |
| 4.4.1. Histological study..... | 19 |
| 5. RESULTS | |
| 5.1 Description of the normal anatomy of synarcual-scapulocoracoid skeleton of the Butterfly ray (<i>Gymnura altavela</i>) based on the CT study..... | 19 |
| 5.2. Description of the traumatic process of the Butterfly ray (<i>Gymnura altavela</i>) based on CT study..... | 22 |
| 5.3. Description of the normal histology of the skeleton of Butterfly ray (<i>Gymnura altavela</i>)..... | 26 |
| 5.4. Description of the histopathology features of the skeleton lesions of the Butterfly ray (<i>Gymnura altavela</i>)..... | 28 |
| 6. DISCUSSION..... | 30 |
| 7. CONCLUSIONS..... | 32 |
| 8. BIBLIOGRAPHY..... | 34 |





1. ABSTRACT

This study investigates the normal anatomy and histology of the spiny butterfly ray (*Gymnura altavela*) through X-ray, computed tomography (CT), and histological samples, focusing on a specific traumatic injury in one specimen. CT analysis highlights key structures, including the scapular girdle and synarcual, illustrating their connections and support for the pectoral fins. Histological findings reveal non-mineralized cartilage, the calcified tesserae layer, and the muscle structure, emphasizing the role of Sharpey's fibers. The examination of the traumatic injury uncovers significant disruption at the synarcual-scapulocoracoid joint, likely caused by a fishing tool. Imaging shows fractures and gas in the wound area, while histological analysis shows tesserae separation, granulocyte infiltration, and fibrous tissue replacing muscle, indicating a chronic response with no cartilage regeneration. The study aims to enhance our understanding of the biology, conservation needs, and health issues affecting the spiny butterfly ray, a species threatened by human activities. It emphasizes the significant impact of these activities on the species' well-being and underscores the urgent need for conservation measures. The findings also highlight the importance of ongoing research into the health issues faced by elasmobranchs, promoting awareness and efforts to protect these remarkable creatures for future generations.

2. INTRODUCTION

2.2 History and Taxonomy

Rays (Cohort Batoidea) and sharks (Cohort Selachii) are part of the group known as elasmobranchs, which fall under the category of cartilaginous fishes or chondrichthyans (class Chondrichthyes). These creatures are distinctively characterized by a skeleton largely comprised of cartilage rather than bone, along with other features that set them apart from other fish. Notably, they lack an operculum and a swim bladder; this absence of a swim bladder necessitates continuous movement in the water column or resting on the ocean floor (Serena et al., 2020). Elasmobranchs are regarded as one of the oldest and most successful lineages of vertebrates, with origins tracing back approximately 400 million years. This group includes the largest and most diverse predatory fishes, boasting around 1,200 species worldwide (Amaral et al., 2018). While rays and sharks evolved from similar ancestors, resulting in some species sharing significant similarities, the anatomy of rays has adapted in ways that further differentiate them from sharks (Last et al., 2016).





The batoid fish group is characterized by a distinctly flattened body, with pectoral fins that are fused to the head and a tail that is narrower than the body. They feature five-gill slits and lack both an anal fin and a nictitating membrane; some species have a venomous sting. The mouth is positioned ventrally, or anteriorly in the case of manta rays, and they possess mosaic-shaped teeth along with spiracles located behind the eyes for water intake (Geraci et al., 2021).

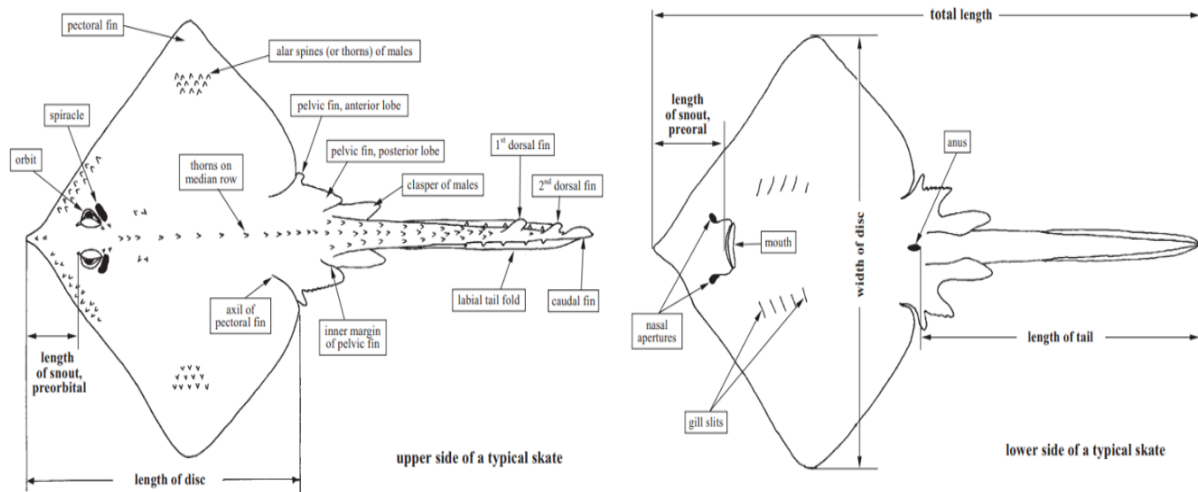


Figure 1. Schematic image of a batoid's dorsal and ventral parts (Bonfil & Abdallah, 2004).

The anatomy of these animals provides valuable insights into their habits and habitats. Their body morphology suggests that, although they are found in both polar and equatorial regions, as well as in coastal areas or at depths of up to 3,000 meters, they primarily have benthic habits. This means they live on the bottom of water bodies, in direct contact with the substrate. This characteristic limits their movement to more diverse geographical areas (Carrier et al., 2012).

These animals play a crucial role in marine ecosystems by regulating the abundance and diversity of plankton, which they feed upon. However, many species are under significant threat and some even face extinction due to their slow growth and late maturation. Their high sensitivity to fishing activities, such as trawling, further exacerbates this issue, making them some of the most threatened species (Geraci et al., 2021).

For years, researchers have studied the classification of these animals. Leonard Compagno conducted a morphological study of elasmobranchs, classifying the Batoidea cohort into four major orders, which are:





Order Torpediniformes (Electric Rays): These species are distinguished by their broad pectoral fins, which are fused with the head and trunk, forming a large, oval disc (Bonfil & Abdallah, 2004). They typically have small or even absent eyes, with certain deep-water species being completely blind. These creatures possess powerful electric organs derived from branchial muscles, which can be observed through the skin as hexagonal macules on both sides of the head. They are primarily found in shallow coastal and tropical-subtropical continental shelf waters across the Atlantic, Indian, and Pacific Oceans. Usually, they inhabit sandy, muddy, and soft substrates, where they often remain buried. However, some species, such as *Torpedo nobiliana*, are known to swim pelagically, even venturing offshore (Ebert & Stehmann, 2013).

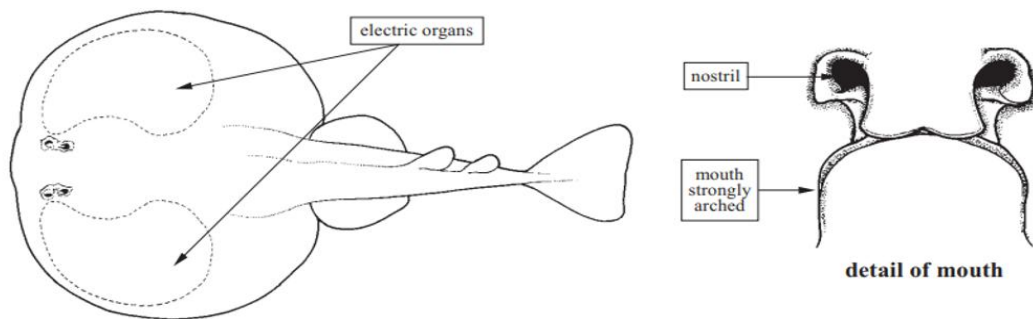


Figure 2. Representative image of an electric ray, F. Torpedinidae (Bonfil & Abdallah, 2004)

Order Pristiformes (Sawfishes): They rank among the largest rays, distinguished by pectoral fins that are not fused to their bodies, which gives them a resemblance to sharks. Their snouts extend forward in a long, flat form, with teeth positioned along the edges like those of a saw (Last et al., 2016). These rays are distributed across the Atlantic, Indian, and Pacific Oceans, primarily inhabiting shelf waters. However, they also inhabit brackish coastal waters and river estuaries, although they seldom venture into freshwater or ascend upstream in rivers (Bonfil & Abdallah, 2004).

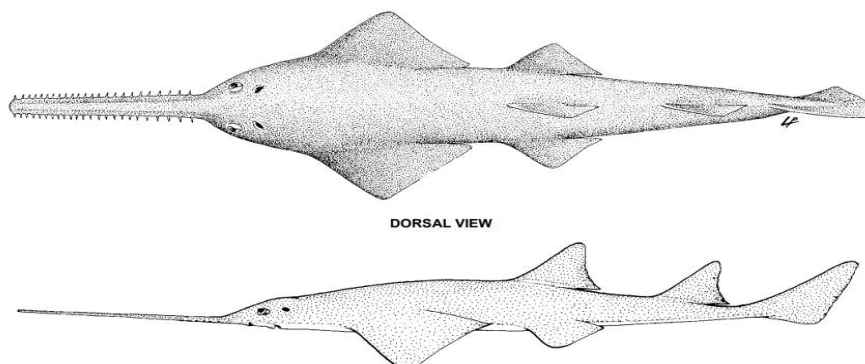


Figure 3. Representative image of a Sawfishes, F. Pristidae (Ebert & Stehmann, 2013).





Order Rajiformes: within this order, we identify three families:

- Rhinobatidae (Guitarfishes): These fish resemble sharks with their elongated body shapes and have gills positioned on the underside of their heads. Their tails are long and robust, featuring two large, separate dorsal fins as well as a prominent, unilateral caudal fin. The snouts are wedge-shaped, supported by a broad and solid rostral cartilage that extends to the tip. Guitarfishes are found in tropical to warm temperate latitudes across all oceans, typically inhabiting the seafloor of continental shelf waters. They swim slowly along the bottom or remain partially buried, occupying depths of up to about 110 meters, and occasionally venture into estuaries and freshwater environments (Ebert & Stehmann, 2013).

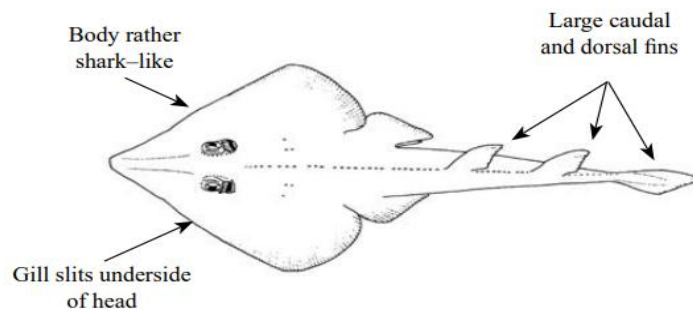


Figure 4. Representative image of a Guitarfishes (Ebert & Stehmann, 2013).

- Rajidae and Arhynchobatidae (Skates): The body is dorsoventrally flattened, featuring very broad pectoral fins that create a disc-like shape, along with small dorsal fins and a rudimentary or absent caudal fin. The snout is characterized by a firm rostral cartilage that extends to the tip. These creatures inhabit exclusively marine environments and can be found in all oceans, ranging from tropical to polar regions, and from shallow coastal areas to abyssal plains at depths exceeding 4,000 meters. They are benthopelagic and are capable of migrating over long distances (Ebert & Stehmann, 2013).

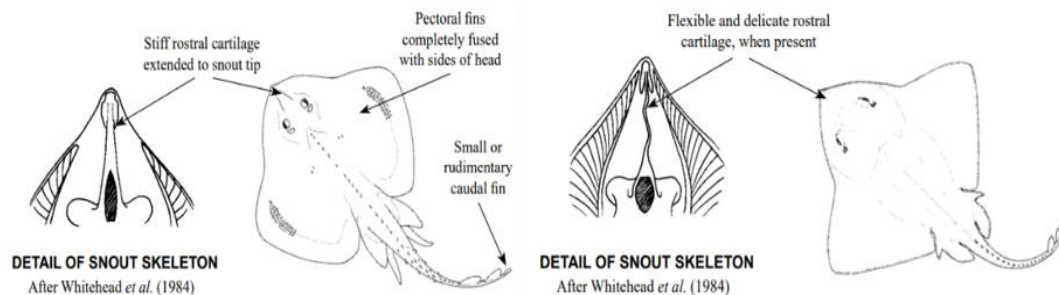


Figure 5. Representative species from two families Rajidae on the left and Arhynchobatidae on the right, highlighting key morphological distinctions (Ebert & Stehmann, 2013)





Order Myliobatiformes: The pectoral fins are fused with the head and trunk, creating a diamond-shaped disc. There is a single dorsal fin that may be present or absent, along with one or more serrated spines or stingers at the base of the upper tail, which can vary in length from very short to long and whip-like. These creatures are distributed worldwide, predominantly in shallow coastal waters that span tropical to warm temperate latitudes, and they can also be found in brackish waters and freshwater estuaries.

Most species are demersal, either residing constantly on the seabed (benthic) or swimming just above it (benthopelagic) (Ebert & Stehmann, 2013). Notably, the group known as mantas is unique in having abandoned the seabed lifestyle, spending the majority of their time swimming near the surface. A total of eleven families are recognized within this group (Hexatrygonidae, Gymnuridae, Plesiobatidae, Urolophidae, Aetobatidae, Rhinopteridae, Mobulidae, Myliobatidae, Urotrygonidae, Potamotrygonidae, and Dasyatidae), with particular emphasis on the Gymnuridae family (Last et al., 2016).

- Gymnuridae (Butterfly rays): Manta rays are large creatures, featuring a wide disc that can reach up to 200 cm in diameter. They possess an extremely short tail and, in most species, one or more long dorsal spines near the base. Notably, they lack both a dorsal and caudal fin, and their snout is very short and angular.

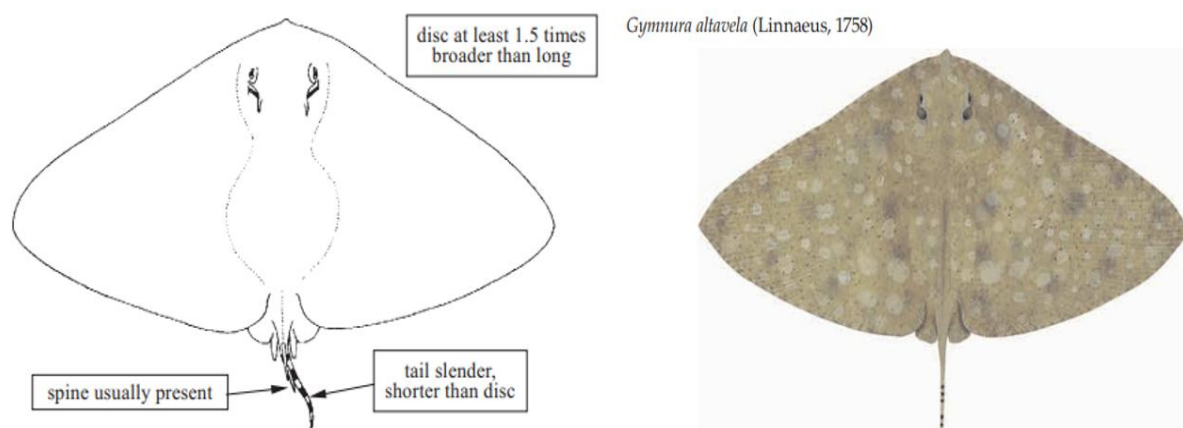


Figure 6. Representative image of a Butterfly ray (Bonfil & Abdallah, 2004), Additionally, it illustrates the distinctive coloration exhibited by this species (Last et al., 2016).





2.3 Description of the ecology of the family Gymnuridae.

Species within the Gymnuridae family, commonly referred to as butterfly rays, exhibit a cosmopolitan distribution across various marine environments, including tropical and warm temperate regions of the Atlantic, Indo-Pacific oceans, and the Mediterranean Sea. These species predominantly inhabit sandy and muddy substrates found in shallow coastal waters, continental shelf zones, lagoons, and estuaries, typically residing at depths ranging from 50 to 100 meters (Ebert & Stehmann, 2013). The Gymnuridae family comprises 14 species within the *Gymnura* genus (Compagno, 1999, 2005). Taxonomic identification of these species relies on specific intraspecific variations, which include the presence or absence of spiracular tentacles, dorsal fins, and caudal stingers, alongside considerations of relative size and the number of black bands present on the tail. Such morphological similarities necessitate detailed examination (Last et al., 2016). Common morphological characteristics of this family include notably large pectoral fins, which can be nearly twice the length of the body, a pronounced dorsoventral compression, and a blunt-angled snout. Additionally, the eyes and spiracles are situated on the dorsal surface of the head, and most species lack fleshy papillae on the oral cavity's floor; furthermore, both surfaces of the disc are typically bare. The coloration of these rays is primarily grayish, ranging from olive brown to dark brown, often exhibiting a mottled pattern on the dorsal aspect of the disc, while the ventral surface is usually characterized by a white coloration (Ebert & Stehmann, 2013).



Figure 7. Morphological Variations within the Genus *Gymnura* (Last et al., 2016).



2.4 Ecobiological description of *Gymnura altavela*

The species *Gymnura altavela* is distributed in the eastern North Atlantic, encompassing regions from the coasts of Morocco and Madeira to northern Portugal and Spain. Its range extends into the Mediterranean and Black Seas, as well as along the western coast of Africa from Angola to the Canary Islands. Additionally, this species inhabits the western North Atlantic, extending from Massachusetts southward through the Caribbean Sea and along the South American coastline to the La Plata estuary in Argentina.



Figure 8. distribution map of *Gymnura Altavela* (Dulvy et al., 2021)

Gymnura altavela typically occupies a benthic habitat, residing on sandy and muddy substrates where it employs a strategy of burial for camouflage and predation on fish, crustaceans, and mollusks. It prefers shallow coastal waters, generally down to depths of approximately 70 meters, although individuals have been recorded at depths of up to 150 meters, indicating demersal behavioral patterns (Ebert & Stehmann, 2013). In terms of reproductive biology, *Gymnura altavela* is characterized as ovoviviparous, with fertilization and embryonic development occurring internally for a duration of 4 to 9 months. Subsequently, parturition results in the birth of 1 to 8 offspring, each measuring between 38 and 44 cm in disc width (Ebert & Stehmann, 2013). Notably, the species does not exhibit significant sexual dimorphism in morphology at birth; newborns present with uniform size and shape. However, as individuals mature, they demonstrate sex-specific growth patterns, with females continuing to grow throughout their lifespan, while males attain an asymptotic size more rapidly (Parsons et al., 2018). Morphologically, the butterfly ray can reach a maximum length of 200 cm. It possesses a disc that is substantially wider than it is long, complemented by an extremely short tail characterized by 3 to 5 dark bands and one or more caudal spines. Adult specimens are noted for a slender tentacle located on the inner margin of each spiracle, directed posteriorly, alongside scattered spines on the upper disc, while juveniles exhibit smooth skin. The lower disc is smooth and white (Last et al., 2016).





2.5 Current situation of the butterfly ray in the world.

The butterfly ray's population has significantly declined across numerous geographic regions, facing an array of anthropogenic threats. These threats include the application of intensive fishing techniques such as trawling, gillnetting, and purse seining, in addition to artisanal fishing practices aimed at commercial exploitation, particularly the international trade of its meat and wings. Moreover, habitat degradation from coastal development, tourism, and pollution worsens the challenges faced by this species.

In the Mediterranean Sea, the species has undergone a significant decline, with no records from Mediterranean trawl surveys (MEDITS) since 1994, indicating a potential disappearance of populations in the northern Mediterranean. In West Africa, reconstructed landing data reveal a notable reduction in catches, further underscoring the population decline. In Brazil, a staggering 99% decrease in the species' abundance has been documented over the last three generations (33 years). These findings suggest an overall population reduction ranging between 50% and 79% throughout its distribution. Globally, *Gymnura altavela* is classified as Endangered; however, regional assessments differ: in the Mediterranean Sea and southwestern Atlantic, it is considered Critically Endangered; in the central and southeastern Atlantic, it is labeled as Endangered; whereas in the northwestern and west-central Atlantic, the species is classified as Least Concern, as it is not commercially exploited in those regions (Dulvy et al., 2021).

Elasmobranchs are especially vulnerable to overfishing due to specific life cycle traits, such as delayed maturation, longevity, and extended incubation and gestation periods. These species face heightened risks of reproductive disorders linked to capture stress, particularly spontaneous abortion, which can result in the premature expulsion of embryos and subsequent reproductive failure (Adams et al., 2018). Given the challenges these species currently encounter and their biological characteristics, there is an urgent necessity to implement targeted conservation measures. These should include species-specific catch landing monitoring, prohibiting the landing of threatened species, sustainable management for all species, accurate identification of at-risk species, enhanced fishery controls and protections, a significant increase in scientific observers to monitor catches, and continued research into gear modifications, fishing practices, and habitat identification to reduce mortality from bycatch and discards among these species (Last et al., 2016).





2.6 Important of the species in the Canary Islands.

Gymnura altavela is classified as Endangered by the IUCN due to overfishing and habitat loss across many areas of its global range. However, the Canary Islands present more favorable conditions for this species. The ban on trawling since 1986 and the fact that local fishers do not target this species contribute to the better conservation of local populations compared to other oceanic regions. The unique geography of the Canary Islands plays a crucial role in the protection of *Gymnura altavela* and many other species. The specific characteristics of the seabed and sandy bottoms provide natural shelter, fostering optimal population development. Additionally, the region boasts high biodiversity, ample food availability, and water temperatures ranging from 19 to 24°C, making it an ideal potential breeding ground for this species (Espino-Ruano et al., 2023). This information is essential for formulating effective conservation measures.

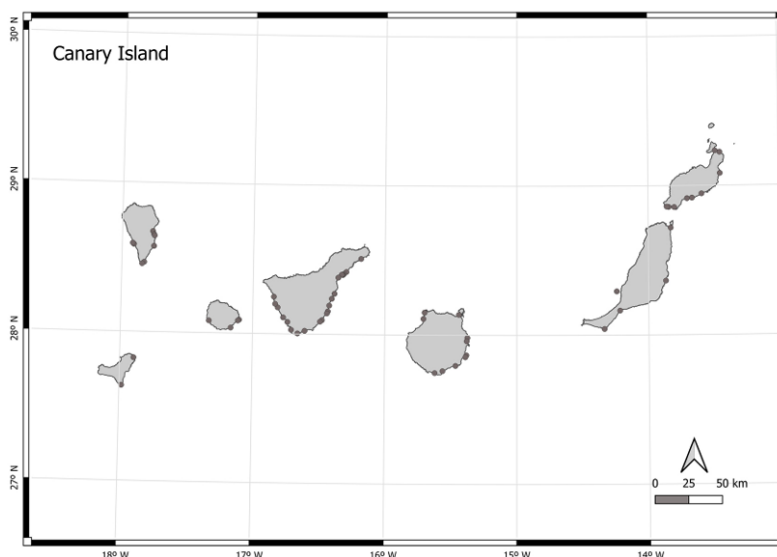


Figure 9. Map of the geographical situation of the Canary Islands, with areas where grey dots represented spiny butterfly rays (Espino-Ruano et al., 2023)

In the Canary Archipelago, several initiatives are dedicated to studying and conserving manta ray populations, notably the CANBIO project and its subproject, BioACU. The primary objective of this initiative is to enhance the acoustic monitoring of marine biodiversity in the Canary Islands through the use of autonomous marine vehicles. The focus is primarily on manta rays and other elasmobranchs, such as the angel shark, to gather comprehensive data on their habitats, movement patterns, and behaviors. This project is a collaborative effort involving the University of Las Palmas de Gran Canaria and the Loro Parque Foundation. Another noteworthy initiative is "Rays of Paradise," led by the Save Our Seas Foundation. This project seeks to broaden the existing understanding of manta rays in the Canary Islands, particularly in





Gran Canaria. Its goal is to gain insights into the distribution and abundance patterns of these species along the island's coastal areas, ultimately providing vital information for improved habitat management. The project incorporates citizen science programs through online databases, along with a visual survey initiative to gather essential ecological information on these rays in Gran Canaria.

The limited knowledge regarding the biology and ecology of certain elasmobranch species, particularly rays, along with the scarcity of fisheries-related research, underscores the importance of citizen science projects for enhancing their understanding and conservation. These initiatives play a crucial role in collecting vital data on distribution, habitat, and population structure. However, many aspects of their biology remain elusive due to challenges such as their size, migratory behavior, and difficulties associated with captivity, which have hindered research efforts. This situation highlights the urgent need for increased studies, especially considering that five of the seven most threatened elasmobranch families are comprised of rays.

2.7 Anatomy and histology of the skeleton of batoid fishes.

Elasmobranchs, which include sharks and rays, possess a skeleton made of cartilage, a strong and durable material that is lighter and more flexible than bone. This unique structure enables them to maintain buoyancy and execute tighter turns compared to other fish, making it the defining anatomical characteristic that distinguishes them. Additionally, they continuously renew their teeth throughout their lives and lack a swim bladder (Long et al., 2024). The skeleton of batoid fishes exhibits specific morphological traits that further differentiate them from other chondrichthyans. These include the presence of the neurocranium, five visible gill slits located on the ventral disc, and the development of the synarcual joint, which supports the pectoral fin by forming the synarcual-scapulocoracoid joint. The pectoral fin is also notable for extending towards both the anterior end (propterygium), reaching the snout, and the posterior end (metapterygium), extending to the pelvic girdle. This unique morphology results in a depressed disc shape, typically wider than long, referred to as the body disc (Cousseau et al., 2007). When these morpho-anatomical features are combined with their lightweight and dynamic cartilaginous skeleton, along with their wing-like pectoral fins, elasmobranchs achieve greater energy efficiency in their swimming movements (Huang et al., 2017).



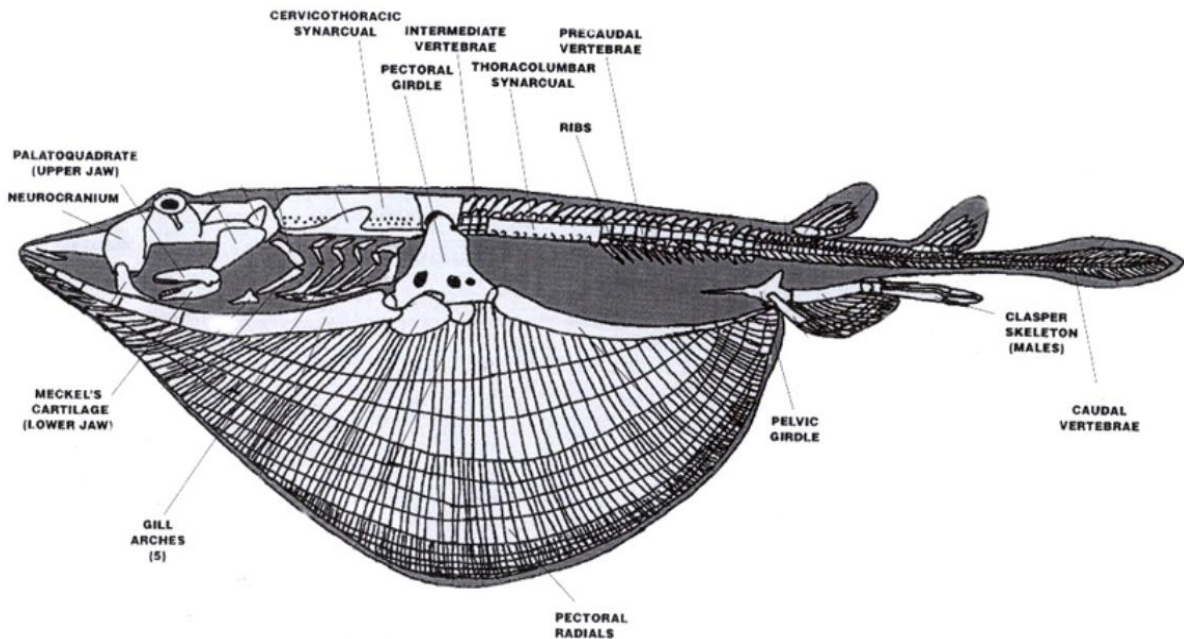


Figure 10. Diagram of an idealized batoid skeleton in lateral view showing the main skeletal structures. Photo modified from *Sharks, Skates, and Rays: The Biology of Elasmobranch Fishes*. 1999. Edited by William C. Hamlett. John Hopkins University Press, Baltimore, Maryland.

The distinguishing characteristics that facilitate the understanding and differentiation of the order Myliobatiformes from other families of rays are comprehensively elucidated herein, with particular emphasis on the attributes of the family Gymnuridae. The morphology of these organisms comprises a disc and a tail; on the dorsal aspect of the disc, one can observe the eyes and spiracles, which serve as the structures for water intake and expulsion when the organism is resting on the benthic substrate. Conversely, the ventral surface of the disc is characterized by the presence of nostrils, the oral cavity, five gill slits, and numerous pores associated with the ampullae of Lorenzini (Cousseau et al., 2007).

The neurocranial anatomy of the Gymnuridae family is primarily made up of pliable cartilage that often undergoes calcification, with degrees of mineralization varying by habitat depth—species in deeper waters tend to be less calcified than those in shallower areas (Fisheries and Oceans Canada, n.d.). The neurocranium is characterized by a flattened, box-like morphology and is devoid of rostral cartilage, a feature that differentiates the Gymnuridae family from others where this cartilage tends to be elongated and robust. Notably, it possesses substantial fontanelle and subdivided postorbital processes (*Gymnura micrura*), which serve as key identifiers within the order Myliobatiformes. However, various studies examining other species within the same family have registered discrepancies in the morphology of the fontanelle and the preorbital





canal, as documented in *Gymnura japonica* (Nishida) and *Gymnura marmorata* (González-Isáis & Domínguez, 2004) (Kobelkowsky, 2017).

The topographical relationships of the neurocranium are delineated as follows: the anterior condyles of the neurocranium articulate with the first proximal radial elements of the pectoral fins; the lateral condyles engage with the antorbital cartilages, while the occipital condyles connect with the synarcual cartilage. This articulation configuration implies that the heads of species within the Gymnuridae family are enveloped by pectoral fins, with radial elements only interrupted near the eyes, before resuming to form the disc (Kobelkowsky, 2017).

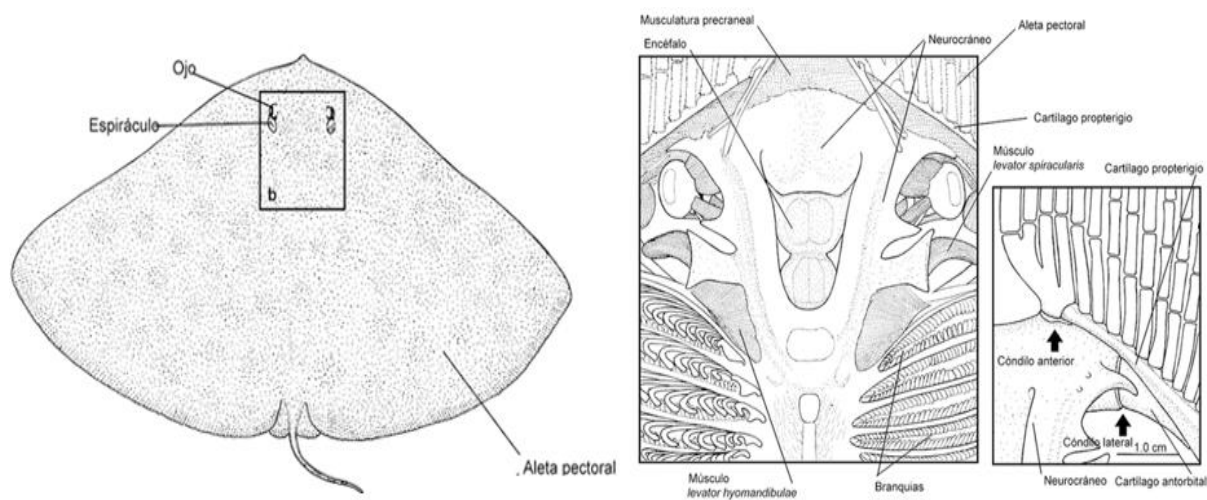


Figure 11. Location of the neurocranium and brain of the butterfly ray *Gymnura micrura*.

Dorsal view of the joint relations of the right olfactory capsule.

Continuing our exploration of the anatomy of this group of animals, we find that posterior to the neurocranium lies the synarcual joint—a crucial structure intimately involved in the movement and support of the pectoral fins. The synarcual is a fusion of several vertebrae in the anterior region of the spine, resulting in a solid cartilaginous formation that provides stability to the front half of the body. It helps maintain the stability of the head and trunk during undulatory swimming, effectively transmitting the forces generated by the movement of the pectoral fins throughout the body. In species belonging to the order Myliobatiformes, the synarcual tends to be larger than in other batoids, owing to its vital role in supporting the notably large pectoral fins characteristic of this group. Additionally, it serves as an anchoring site for several important muscles, including those that control pectoral fin movement, enabling complex and efficient maneuvers in the water (Nishida, 1990).



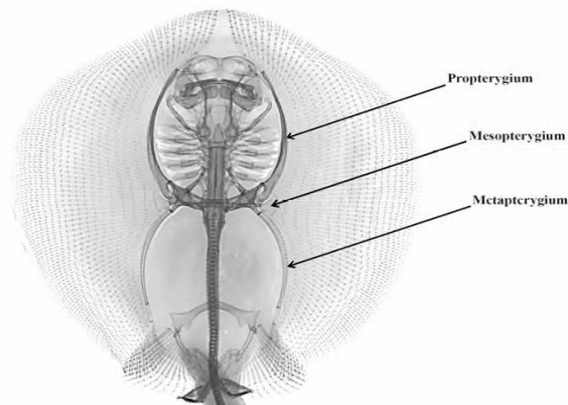


Figure 12. Skeletal structure. Representative batoid (*Urobatis maculatus*) to display the three primary cartilages: propterygium, mesopterygium, and metapterygium which support the pectoral fin. We can also observe the synarcual articulation. (Hall et al., 2018)

This rigid platform connects the spine to the scapulocoracoid complex, forming the synarcual-scapulocoracoid joint, which is vital for the mobility and support of the pectoral fins, facilitating the undulatory propulsion of rays. The scapulocoracoid joint comprises the coracoid cartilage along with the scapular and suprascapular processes. The dorsoventrally flattened coracoid cartilage is positioned beneath the synarcual, providing support to the pectoral fins, while the scapular process articulates securely with the lateral side of the synarcual, enhancing the mobility and support of the pectoral fins. Openings known as fenestrae are present on the lateral surface of the scapulocoracoid, allowing for the passage of muscles and nerves. Additionally, the propterygium, mesopterygium, and metapterygium play significant roles: the propterygium articulates with the anterior corner of the scapulocoracoid and extends anteriorly to the anterior condyles of the neurocranium, while the mesopterygium and metapterygium lie along horizontal axes in relation to the scapulocoracoid. Together, these three pterygiophores, along with the scapulocoracoid, provide essential support to the pectoral radials (Nishida, 1990).

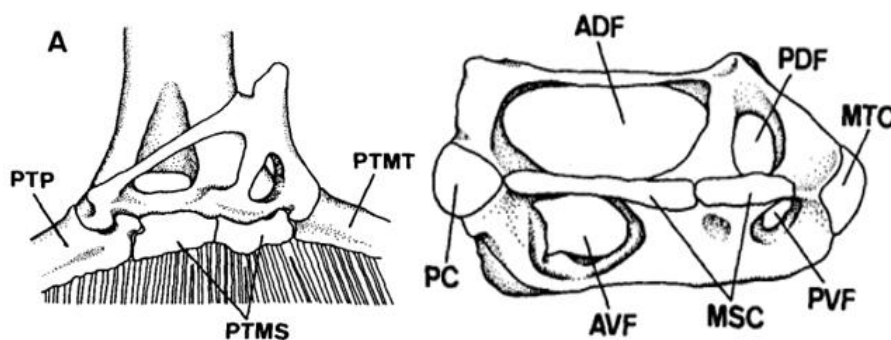


Figure 13. Scapulocoracoid joint (*Gymnura japonica*). In the dorsal (left) view: PTP, pectoral propterygium; PTMS, pectoral mesopterygium; PTMT, pectoral metapterygium. In the lateral (right) view: ADF, anterodorsal fenestra; AVF, anteroventral fenestra; MSC, mesocondyle; MTC, metacondyle; PC, procondyle; PDF, postdorsal fenestra; PVF, postventral fenestra (Nishida, 1990).





At the macroscopic level, pectoral fins are characterized by a hierarchical structure of fin rays, which themselves consist of radial elements interconnected by joints. At the microscopic level, the fin rays bifurcate into two branches at approximately two-thirds the length of the proximal region. The positioning of the joints varies among the rays; as one moves closer to the distal region, the joint positions become increasingly offset, allowing for enhanced kinematic movements. The middle section of each radial element is composed of three chains of tesserae—mineralized cartilage embedded within non-mineralized cartilage. The ends are highly mineralized, serving as structural points of support.

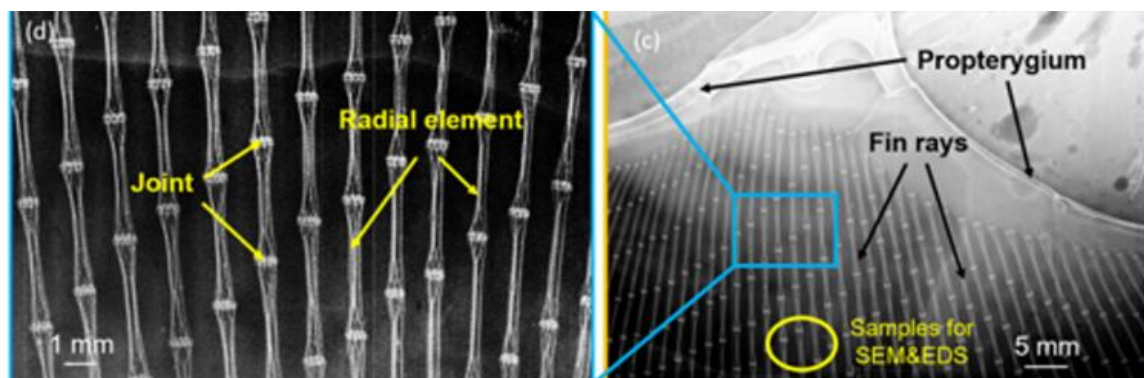


Figure 14. X-ray image of the structure of the pectoral fin and the radial elements separated by joint (Huang et al., 2017).

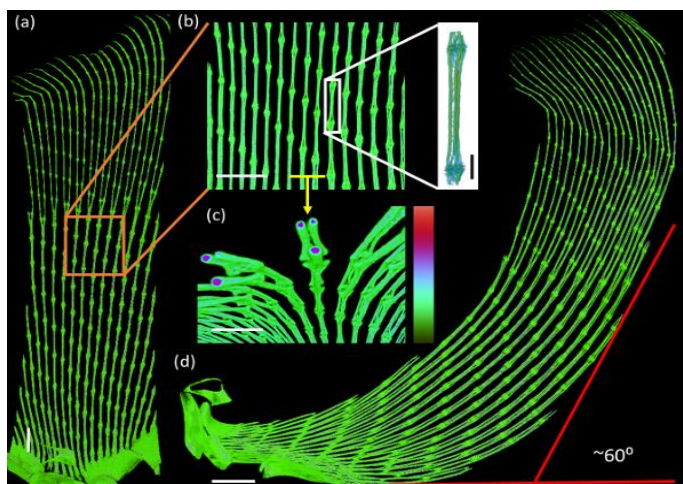


Figure 15. Micro-computed tomography images of radii and radial elements; Cross-section of radial element, showing three mineralized components in each element. The green color has a lower mineral density, the red color has a higher mineral density (Huang et al., 2017).

Each tesserae chain is enveloped by the perichondrium, which provides essential nutrients to the cartilaginous tissue and features aligned collagen fibers that wrap circumferentially around the chains. These radial components are also composed of calcium and phosphorus in a low ratio, indicating that the mineral present is likely biphasic calcium phosphate. Furthermore, these radial structures are encased in muscle fibers. This entire architecture enhances the





distribution of shear, tensile, and compressive stresses, facilitating improved support for lifting and thrust forces during swimming, all while maintaining flexibility (Huang et al., 2017).

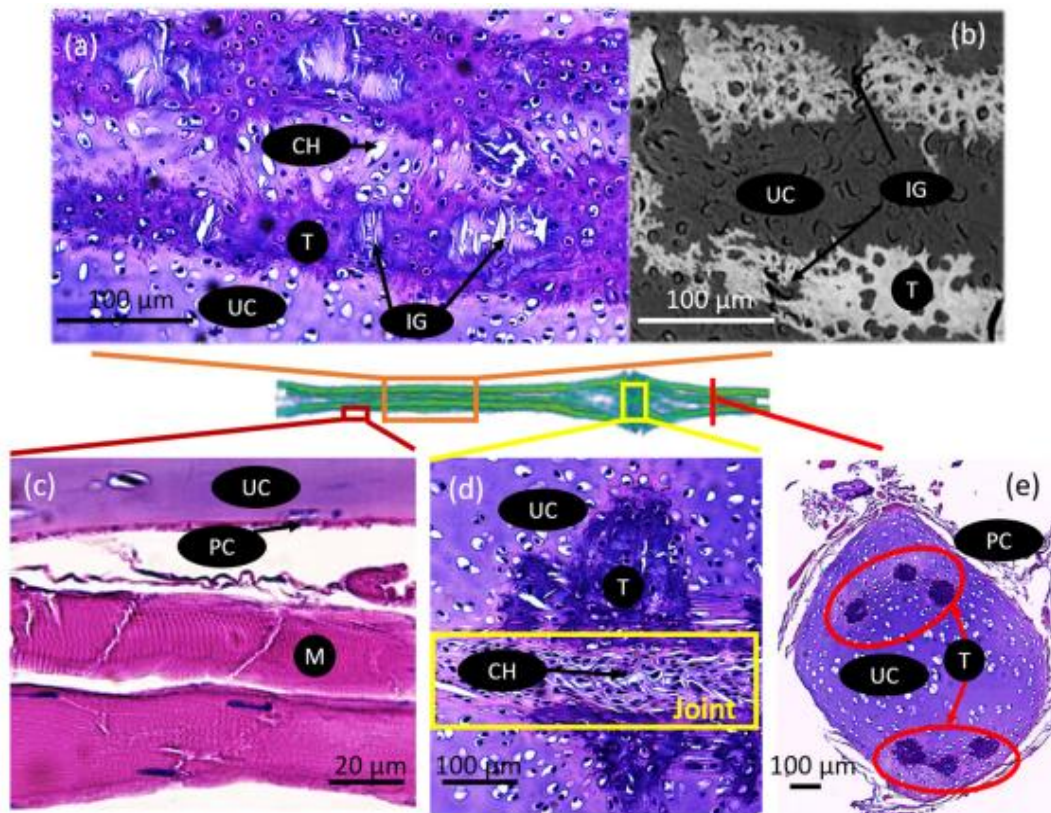


Figure 16. Optical microscopy images of hematoxylin and eosin stained fin radial element sections. CH, chondrocytes. T, tesserae. UC, unmineralized cartilage. IG, unmineralized tissue is shown in the gap between the tesserae. M, muscle fibers. PC, perichondrium (Huang et al., 2017).

3. OBJECTIVES

The first objective of this study is to provide a comprehensive description of both the macroscopic and microscopic characteristics of the normal osteology of the synarcual-scapulocoracoid joint of the *Gymnura altavela*. The second is to provide a comparison with the synarcual-scapulocoracoid joint that has suffered anthropogenic trauma.

This work will allow us to identify key differences that will help to recognize trauma in future research. In addition, it will contribute to expanding knowledge of elasmobranchs, particularly within the poorly researched group of batoid fishes, which face significant threats. In doing so, we hope to support future studies related to the pathology, conservation and ecobiology of living populations.





4. MATERIALS AND METHODS

4.1 Origins of the Specimens

This study focuses on the analysis of two female specimens from the order Myliobatiformes, specifically the species *Gymnura altavela*, commonly known as the spiny butterfly ray. One of the females (SA1087-22) serves as a reference specimen representing a healthy individual, acting as a control for comparison with the histological findings from the second female (SA171-23). The latter specimen was observed near the Castillo del Romeral pier in Gran Canaria (Canary Islands, Spain), resting on the sandy bottom, and exhibited a circular incised-contused traumatic lesion measuring 2 cm in diameter on the scapulocoracoid cartilage (Figure 17), the specimen was transported to the facilities of the Poema del Mar Aquarium (Loro Parque Fundación, Gran Canaria), where a radiological examination was carried out to evaluate the affected structures and ascertain the depth of the lesion (Figure 18). Four days later, the specimen (SA171-23) unfortunately passed away and was subsequently transferred to the Institute of Animal Health and Food Safety (IUSA) at the University of Las Palmas de Gran Canaria (ULPGC) for further investigation. At IUSA, a computed tomography (CT) scan was conducted, followed by a necropsy at the University Veterinary Hospital.

Table 1. Origin of the specimens

| ID | Origin | Description | Test carried out | Animals |
|-----------|--|---|--|----------------------------------|
| SA1087-22 | Specimen from a private center in Gran Canaria | Female | Postmortem CT scan, and standard necropsy. | Healthy animal used as a control |
| SA171-23 | Specimen found at Castillo del Romeral pier in Gran Canaria. | Female Weight: 32 kg Disc width of 179 cm. Total length of 114 cm. | Antemortem X-ray; Postmortem CT scan and standard necropsy. | Animal with Traumatic Pathology. |





Figure 17. Dorsal view of the disc of the specimen (SA171-23), a female *Gymnura altavela*. The pectoral arch of the skeleton (indicated by the white arrow) and a notable concavity on the dorsal surface of the coelomic cavity (indicated by the black arrow) are both visible, resulting from the animal's cachectic condition. Inset: a detailed view of the penetrating, incised-contused wound, illustrating erythema, congestion, and edema at the edges of the injury.

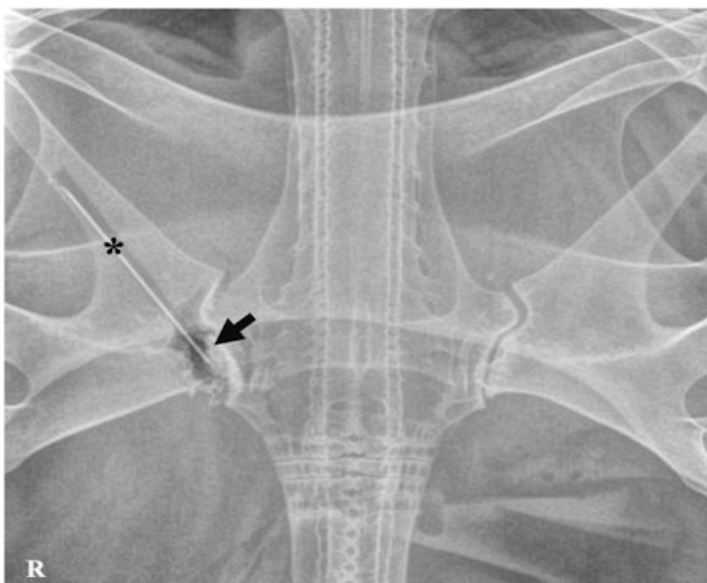


Figure 18. Dorsoventral view of X-ray of the spiny Butterfly ray (*Gymnura altavela*) (SA171-23). During the X-ray examination, a needle with a cap (*) was strategically inserted to enhance the visualization of the incised-contused wound. The black arrow delineates the precise location of the lesion, which exhibits irregular margins accompanied by gas opacity.



4.2 Macroscopical Assessment

Imaging test performed

For the postmortem study, Computed Tomography (CT) was performed in both specimens (SA1087-22; SA171-23), and sequential slices were obtained using a 16-slice helical CT scanner (Toshiba Astelion, Canon Medical System®, Tokyo, Japan). The animals were symmetrically positioned in dorsal recumbency on the stretcher, with craniocaudal entry, and a standard clinical protocol was used (120 kVp, 50 mA, acquisition matrix of 512 x 512, field of view of 1809 x 834, pitch of 0.94, and a gantry rotation of 1.5 s) to acquire images of 1 mm thickness. Different CT images were obtained in dorsal, transverse, and sagittal planes with bone and soft tissue windows. All these images were uploaded to an image viewer (OsiriX MD, Apple, Cupertino, CA, USA) to perform data manipulation.

Necropsy procedure

A necropsy is defined as the procedure in which the systematic postmortem study of an animal's body is carried out through the meticulous dissection of each of its parts (Gázquez, 1989). The aim is to obtain information on the anatomy and biology of the specimen, as well as any diseases it suffered from and the cause of death. Under the established protocol, the reception data for the specimens were initially documented, capturing details such as origin, sex, date of death, clinical findings related to the body, geographical location, and the methods employed for preservation and transport. Subsequently, biometric data were gathered, which included age, morphology, and morphometry, categorized as juvenile, young, or adult. A thorough examination followed, consisting of both external and internal assessments. During the external examination, injuries and abnormalities were meticulously evaluated, with a detailed description provided for the wound observed in the scapulocoracoid cartilage. The internal examination was conducted with the specimen positioned supine, involving ventral incisions to allow for the extraction and further evaluation of the organs. Samples were preserved in a 10% formalin solution to enable comprehensive histological, toxicological, and microbiological analyses. In our case, samples were taken from the wound and the main organs for histopathological examination; to allow a comparison between the normal and affected cartilage, a sample of unaffected scapulocoracoid cartilage was also taken.





4.4 Microscopical Assessment

4.4.1 Histological study

To analyze the cartilage tissue samples, they were initially subjected to a histological decalcifier (Decalcifier DC2, Qpath®, Fontenay-sous-Bois, France) for 7 days. Following fixation, the samples were placed in cassettes and underwent routine processing, which included dehydration through ascending grades of alcohol, clearing in xylene, and embedding in paraffin. The paraffin blocks were subsequently sectioned at a thickness of 4 µm and stained with hematoxylin and eosin (H&E), periodic acid-Schiff (PAS), and Masson's trichrome (MT). Finally, the slides were mounted and examined using a light microscope (Olympus BX51, Tokyo, Japan), which was equipped with DP21 camera software (Olympus DP21, Tokyo, Japan).

5. RESULTS

5.1 Description of the normal anatomy of synarcual-scapulocoracoid skeleton of the Butterfly ray (*Gymnura altavela*) based on the CT study.

CT has proven to be an invaluable tool for studying anatomy and facilitating the evaluation of bones, organs, and tissues for diagnostic purposes. A CT scan was conducted on a healthy specimen (SA1087-22) to document the normal anatomy of a *Gymnura altavela*, which will serve as reference material for examining specimen (SA171-23), known to present a lesion in the synarcual-scapulocoracoid joint, the focus of this study. We aim to enhance our understanding of this anatomical region by utilizing various CT sections. In (Figure 19), the topography and components of the pectoral girdle and surrounding structures are displayed from a dorsal view, showcasing the synarcual, scapular process, suprascapula, coracoid cartilage, and the pterygiophores—propterygium, mesopterygium, and metapterygium. Collectively, these structures provide essential support to the pectoral fins.

The description of the synarcual structure begins with its articulation with the neurocranium, as illustrated in (Figure 20.A). This articulation is facilitated by the occipital condyles present in both cartilages. The synarcual is an elongated cartilage that comprises 28 to 30 vertebral segments, as evidenced by the spinal nerve foramina, which remains obscure due to the subtle dorsal curvature of the synarcual base. The neural canal extends dorsoventrally, forming a crest with broad walls and a ventral base, accommodating the substantial size of *Gymnura altavela*. Notably, the anterior opening of the neural canal takes on a teardrop shape, projecting forward





to create a "lip" that resides within the foramen magnum of the neurocranium (Claeson, 2008). The pectoral arch plays an important role in the formation of the pectoral girdle, as depicted in (Figure 21), the pectoral arch is positioned on the dorsal surface of the synarcual. The anterior margin of the pectoral arch is broader and extends laterally, forming the synarcual's articular surface, which connects with the suprascapula via the scapular process, thereby establishing the synarcual-scapulocoracoid joint.

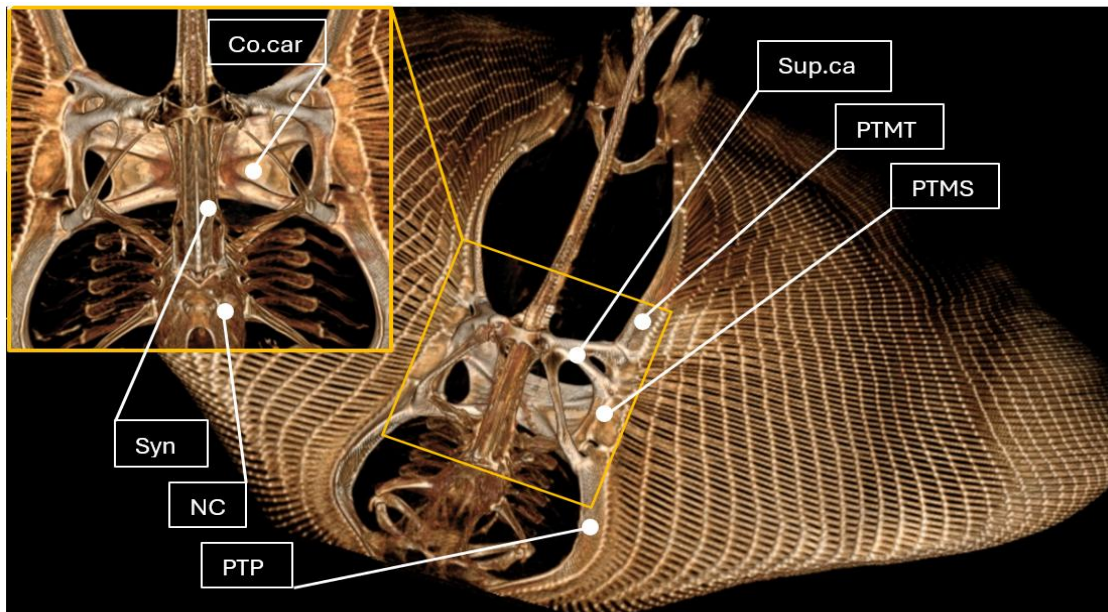


Figure 19. A computed tomography (CT) scan of the *Gymnura altavela* specimen (SA1087-22). Dorsal view of the complete skeletal synarcual-scapulocoracoid structure. Abbreviations: Co.car – coracoid cartilage; NC – neurocranium; PTP – propterygium; PTMS – mesopterygium; PTMT – metapterygium; Syn – synarcual; Sup.ca – suprascapular.

The suprascapula, along with the coracoid, contributes to the formation of the scapulocoracoid cartilage, which typically exhibits a subrectangular shape when viewed laterally in most myliobatidoids. However, as illustrated in (Figure 20.B), it is more anteroposteriorly elongated in the *Gymnura* family. The suprascapula articulates with the synarcual through the scapular process, and at its most distal end, it connects to the pterygiophores via condyles: the procondyle for the propterygium, the mesocondyle for the mesopterygium (which, in the case of *Gymnura altavela*, comprises two), and the metacondyle for the metapterygium, as shown in (Figure 20.B) (Nishida, 1990). The pterygiophores articulate with the distal region of the suprascapula, contributing to the disc shape of the *Gymnura altavela* body and supporting the radials that form the fins. The coracoid cartilage is flattened and located beneath the synarcual, providing structural support to the pectoral fin and scapular process.



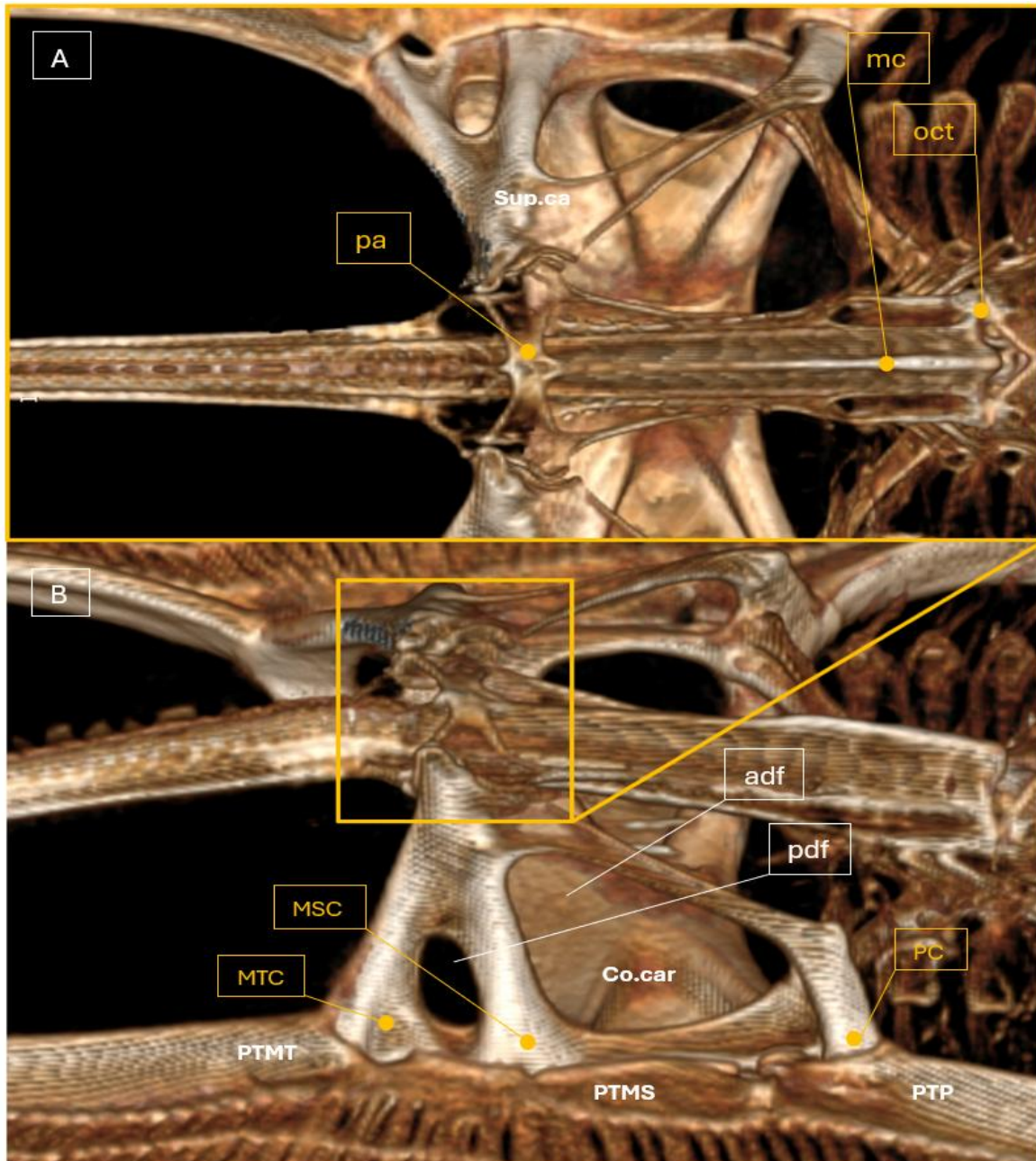


Figure 20. CT scan of the skeleton of the *Gymnura altavela* (SA1087-22). A: dorsal view of the synarcual-scapulocoracoid joint, where we can observe the pectoral arch and how it is articulated with the suprascapula. B: Dorsolateral view of the synarcual-scapulocoracoid joint shows the scapulocoracoid cartilage and its interaction with the propterygium, mesopterygium, and metapterygium of the pectoral fin. Abbreviations: adf – anterodorsal fenestra; Co.car – coracoid cartilage; MSC – mesocondyle; MTC – metacondyle; mc – median crest; oct – occipital condyle; pa – pectoral arch; PTP – propterygium; PTMS – mesopterygium; PTMT – metapterygium; PC – procondyle; pdf – postdorsal fenestra; Sup.ca – suprascapular.



In (Figure 20.B), we can observe the fenestrae located on the lateral surface of the scapulocoracoid. *Gymnura altavela* features a prominent anterodorsal fenestra situated above the scapulocoracoid condyles, which is the largest of its kind, along with an anteroventral fenestra located beneath the scapulocoracoid condyles. Additionally, there are two smaller posterior fenestrae, one positioned dorsally and the other ventrally. These fenestrae facilitate the attachment of fin musculature to the pectoral girdle (Nishida, 1990).

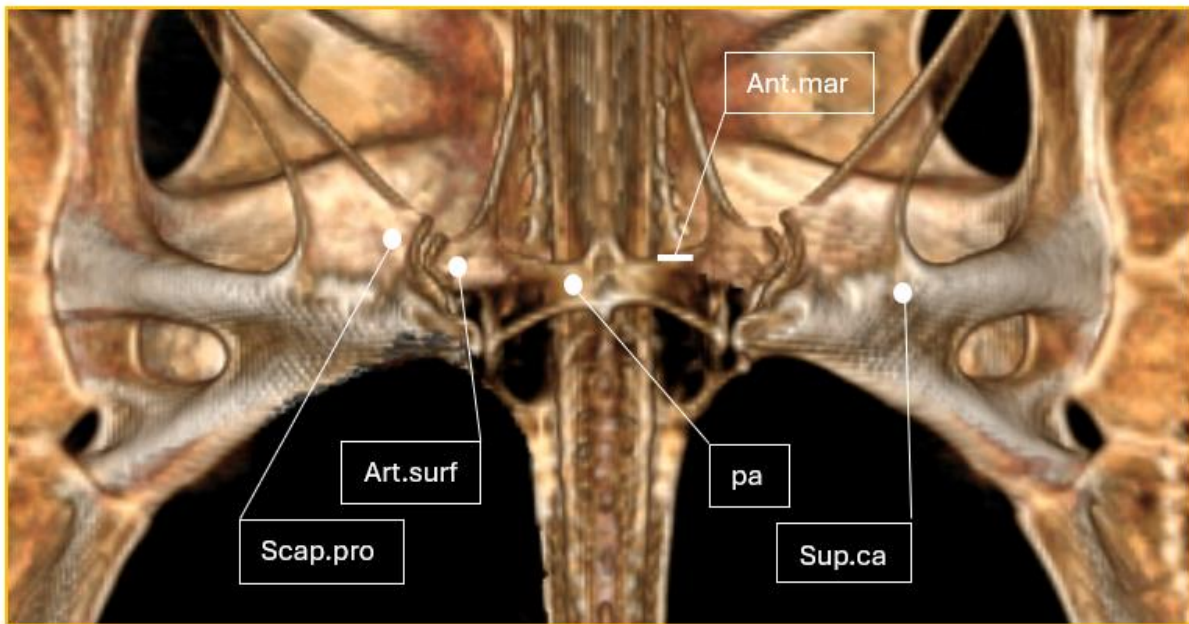


Figure 21. CT scan of the skeleton of the *Gymnura altavela* (SA1087-22). Dorsal view of the synarcual-scapulocoracoid joint. Abbreviations: Ant.mar – anterior margin; Art.surf – articular surface; pa – pectoral arch; Scap.pro – scapular process; Sup.ca – suprascapular.

5.2 Description of the traumatic process of the Butterfly ray (*Gymnura altavela*) based on CT study.

To gain a deeper understanding of the injury's extent (SA171-23), a CT scan was conducted, which revealed the significance of the damage. The diverse array of tools and functionalities provided by computed tomography (CT) enabled us to systematically assess the structural integrity of the bodily components, facilitating a comprehensive evaluation of the extent of damage sustained. In (Figure 22.C) we use a bone window and a cross-sectional image, that illustrates that in the dorsal region of the synarcual-scapulocoracoid joint, there is a visible discontinuity in the skin characterized by irregular borders and a clear presence of gas. This gas is concentrated in the injured area and extends into the ventral region of the synarcual.



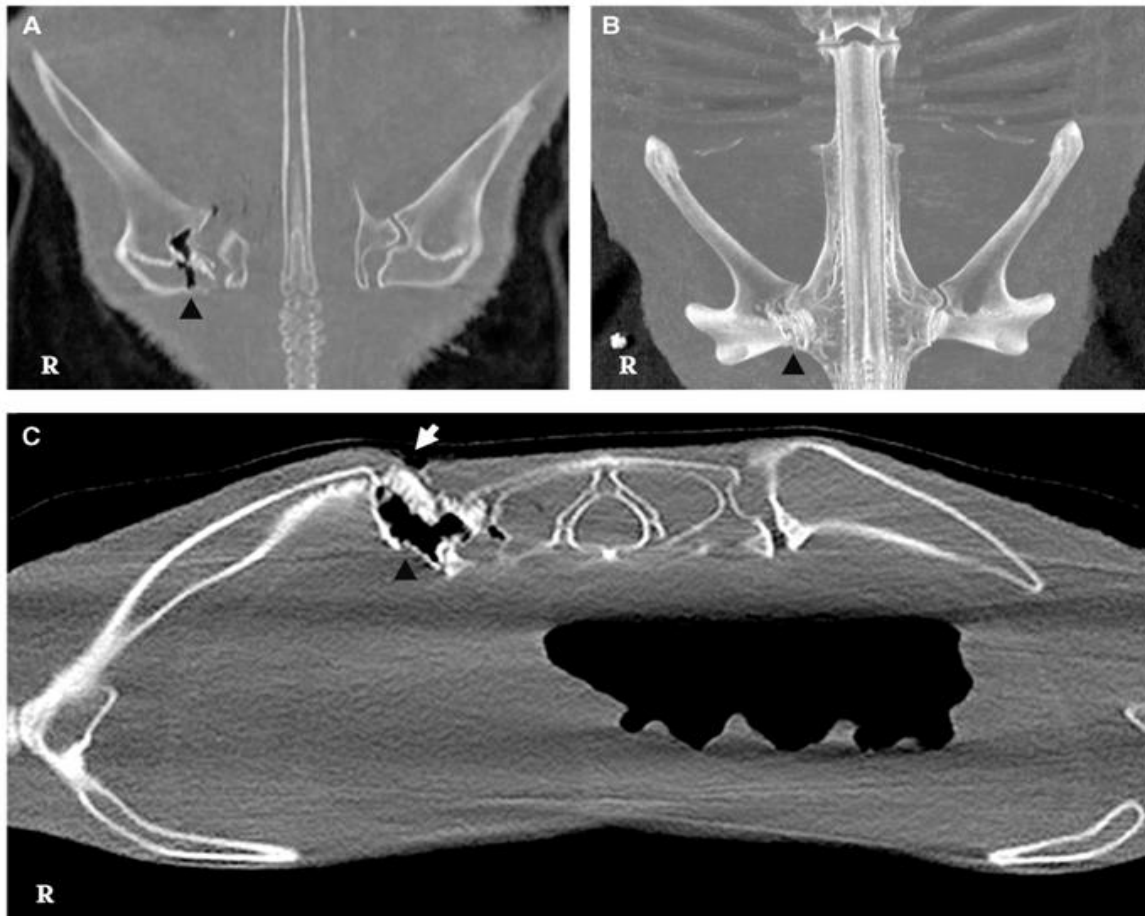


Figure 22. CT scan of the spiny Butterfly ray (*Gymnura altavela*) (SA171-23). A, B: In the dorsal view of the scapular belt, the middle zone of the scapulocoracoid cartilage exhibits irregular edges. Notably, there is a slight attenuation of gas in this region, as indicated by the black arrow. C: In the cross-sectional imaging, notable findings are observed in the dorsal region of the synarcual-scapulocoracoid joint. There is a discernible discontinuity of the skin, as indicated by the white arrow, which is characterized by irregular margins and the presence of gas opacity, highlighted by the arrowhead.

In continuing our descriptive study of the traumatic injury, we aimed to understand how the cartilaginous skeleton of *Gymnura altavela* was impacted. We obtained a series of 3D images through the CT scan conducted on specimen (SA171-23). As illustrated in (Figure 23.A), the junction of the suprascapula with the pectoral arch is highlighted by the white rectangle. This area exhibits irregularities on its dorsal surface, indicating the point of impact with a sharp object. The dorsolateral view of the skeleton confirms that only this region of the scapular girdle sustained damage. Additionally, (Figure 23.B) presents a lateral view of the skeleton, revealing the fenestrae in their entirety, with no other signs of damage evident.

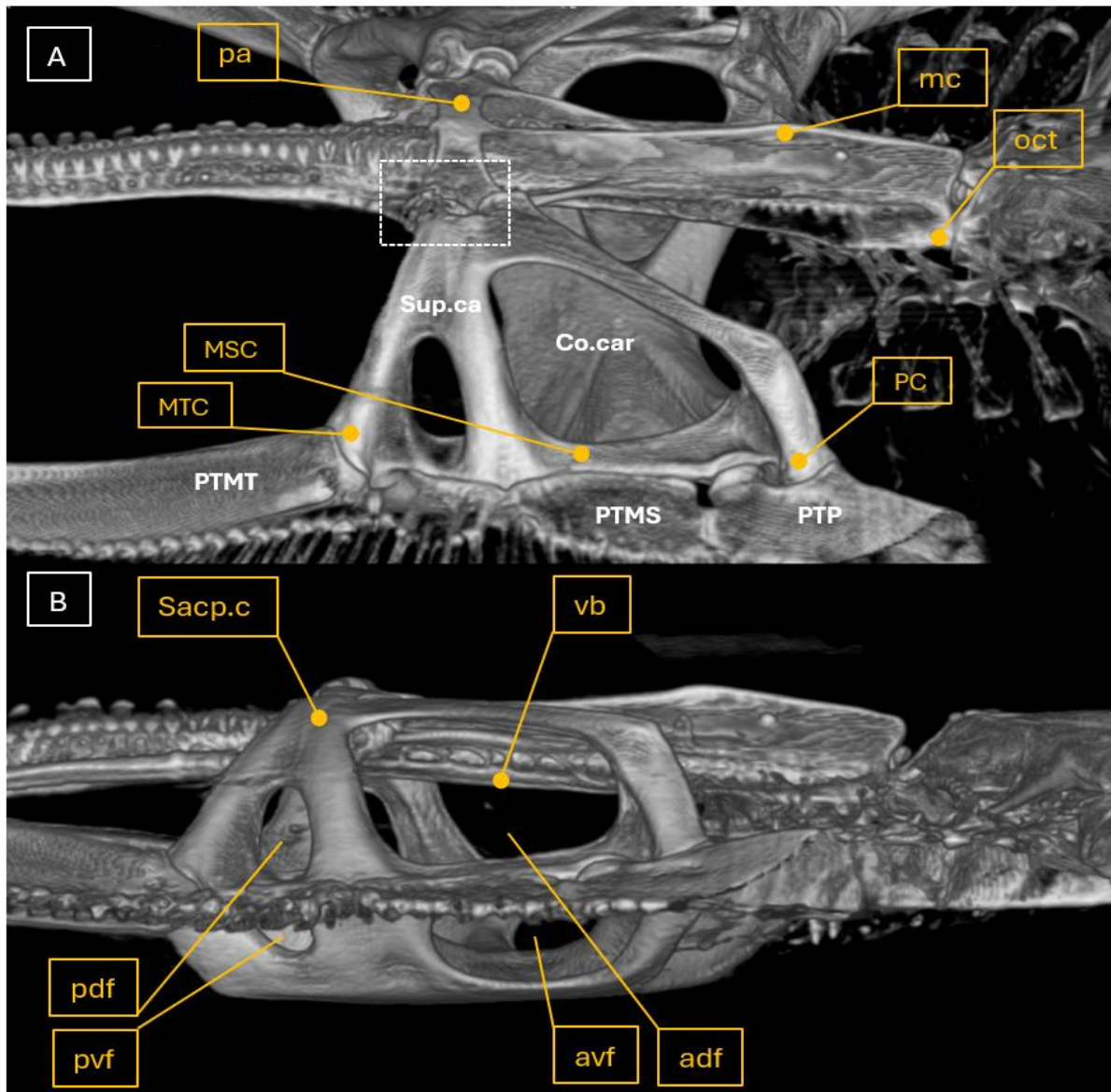


Figure 23. CT scan of the skeleton of the *Gymnura altavela* (SA171-23). A: dorsolateral view of the synarcual-scapulocoracoid joint. This perspective allows for examining the articular surface of the scapulocoracoid cartilage as it interfaces with the principal cartilage components of the pectoral fin, specifically the propterygium, mesopterygium, and metapterygium. B: lateral view of the synarcual-scapulocoracoid joint, where we can observe the fenestras for the passage of the muscle that gives mobility to the fin. Abbreviations: adf – anterodorsal fenestra; avf – anteroventral fenestra; Co.car – coracoid cartilage; MSC – mesocondyle; MTC – metacondyle; mc – median crest; oct – occipital condyle; pa – pectoral arch; PTP – propterygium; PTMS – mesopterygium; PTMT – metapterygium; PC – procondyle; pdf – postdorsal fenestra; pvf – postventral fenestra; Sacc.c – scapulocoracoid; Sup.ca – suprascapular; vd – ventral base. White rectangle: Injury.



After conducting a comprehensive study of the scapular girdle, the focus was narrowed to the synarcual-scapulocoracoid joint (Figure 24.A), which illustrates in detail the impact on both the suprascapular structure and the synarcual articular surface. A closer inspection of the injured area depicted in (Figure 24.B) shows a loss of the anatomical shape in the most proximal region of the suprascapula. In comparison to the left joint (the twin joint), it becomes apparent that the joint on the right lacks of the scapular process, a discernible articular edge, condyle, or fossa. Instead, both articular surfaces appear to merge into a single, highly irregular, and depressed structure.

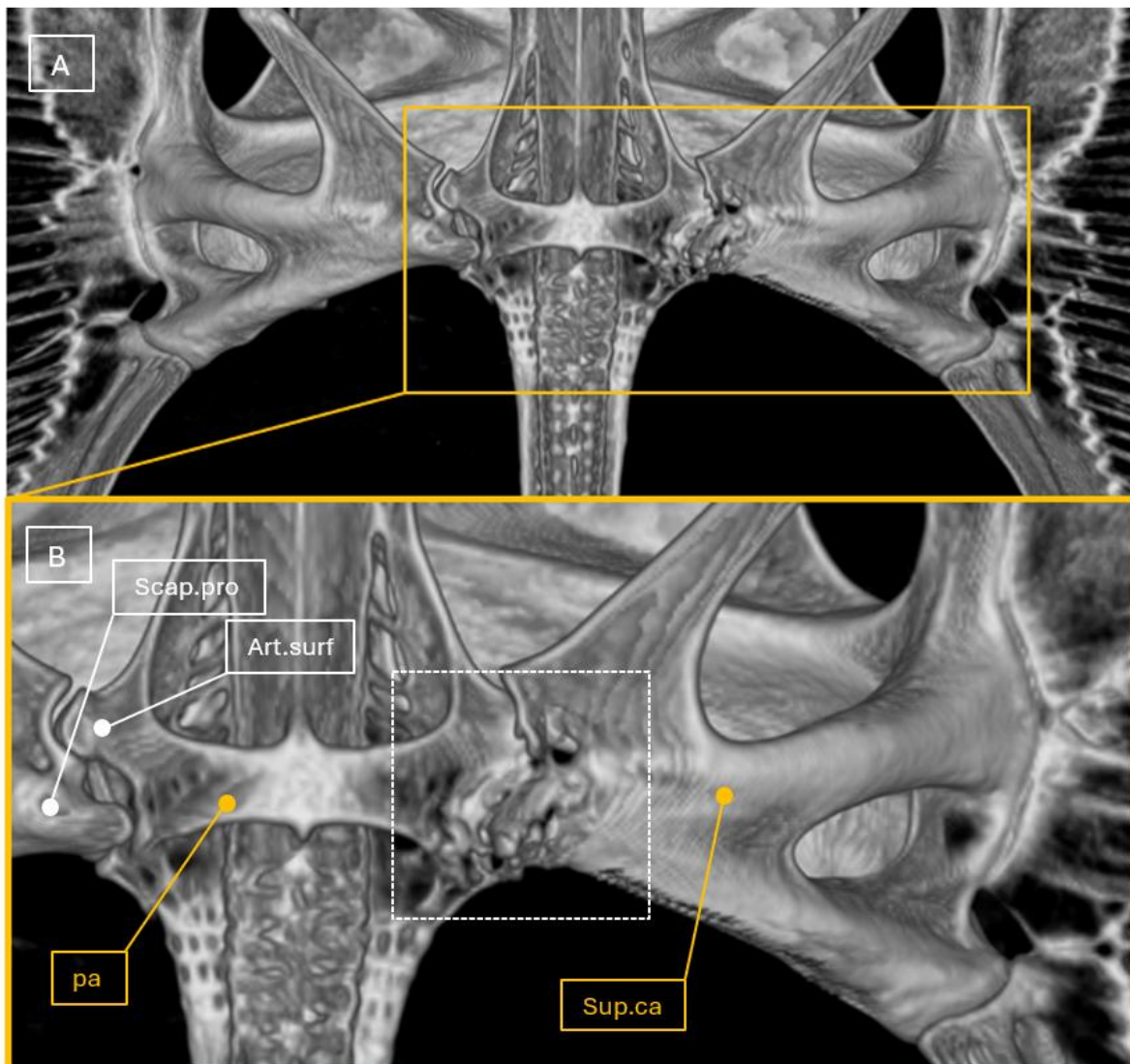


Figure 24. CT scan of the skeleton of the *Gymnura altavela* (SA171-23). A: dorsal view of the synarcual-scapulocoracoid joint. B: closeup of the synarcual-scapulocoracoid joint. Abbreviations: Art.surf – articular surface; pa – pectoral arch; Scap.pro – scapular process; Sup.ca – suprascapular. White rectangle: Injury.





5.3 Description of the normal histology of skeleton of the Butterfly ray (*Gymnura altavela*)

To enhance our understanding of the lesion being studied, we will first describe the normal histology of the cartilaginous skeleton of the spiny Butterfly ray (*Gymnura altavela*). This foundational knowledge will aid in comprehending the histopathology of the lesion later on. The histological samples referenced were obtained from specimen (SA171-23), specifically from the scapula-coracoid joint, which displayed no visible lesions, thereby illustrating a normal cartilaginous structure, as depicted in (Figure 25). We will begin by emphasizing the unmineralized cartilaginous core, which is encircled by a layer resembling dark pink polygonal tiles that correspond to the tesserae. This arrangement forms a calcified outer ring that provides support and rigidity to the cartilaginous skeleton. The tesserae are enclosed by the fibrous perichondrium, and all of these structures are covered by the muscular layer.

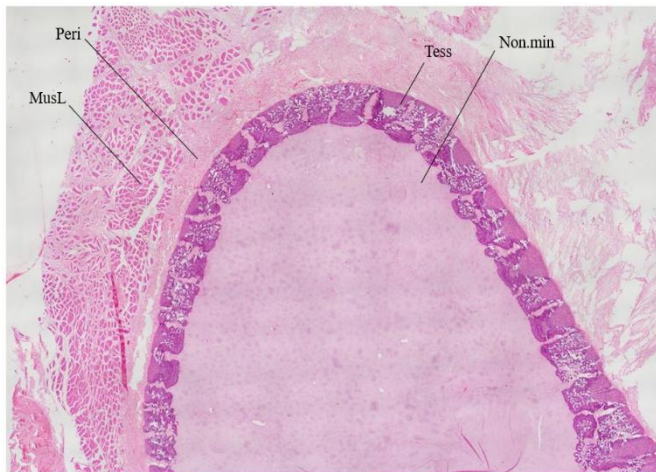


Figure 25. Histological examination. Illustrates the normal architecture of cartilage, highlighting several structural components. Abbreviation: MusL – muscle layer; Non.min – non-mineralized cartilage core; Peri – perichondral region; Tess – tesserae layers. The tissue was stained using hematoxylin and eosin (H&E) to facilitate these observations.

Recognizing the vital role of the tesserae layer, we analyzed it at higher magnifications as shown in (Figure 26). The cells that make up the cartilage are referred to as chondroblasts, which are responsible for synthesizing the surrounding matrix. This matrix ultimately encases the chondroblasts, creating lacunae and transforming them into chondrocytes. The tesserae undergo a more extensive calcification process, which accounts for their darker pink coloration. The perichondrium comprises mesenchymal cells and serves to nourish the adjacent tissue. As these cells differentiate into chondroblasts and produce the surrounding matrix, they become avascular and aneural, playing a crucial role in skeletal growth (Johanson et al., 2019). Additionally, in (Figure 26), we can observe Sharpey's fibers, these collagen fibers, located in cartilaginous tissue, extend from the perichondrium into the matrix, primarily securing the perichondrium to the tesserae layer and providing supplementary support.



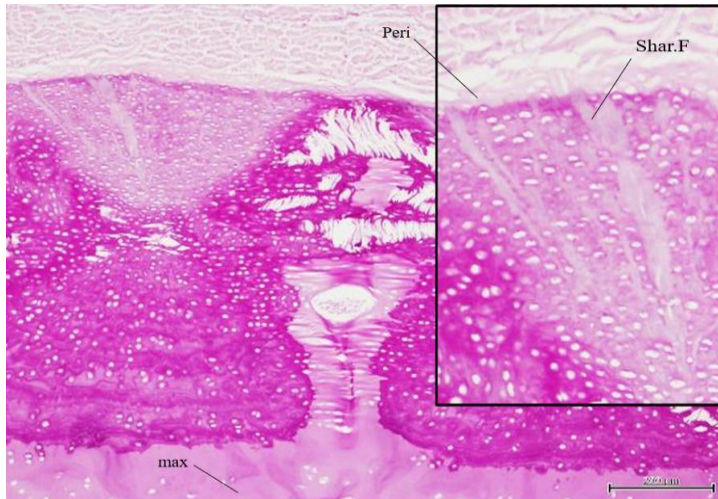


Figure 26. The normal architecture of the tesserae is evident, along with Sharpey's fibers from the perichondrium penetrating the tesserae layer. Abbreviation: max – matrix; Peri – perichondral; Shar.F – Sharpey's fibers. Periodic acid-Schiff (PAS) staining was utilized for visualization.

Hematoxylin and eosin (H&E) staining was applied for (Figure 25), while Periodic Acid-Schiff (PAS) staining was utilized for (Figure 26). Additionally, Masson's trichrome (MT) staining was performed (Figure 27), in which the perichondrium was stained blue, effectively distinguishing it from the more reddish muscular layer. In the same way, the peripheral edges of the tesserae pieces (Figure 27.B) were differentiated from the intertesseral fibrous zones (ITZ). This staining technique enhanced the visualization of the various collagen fibers present.

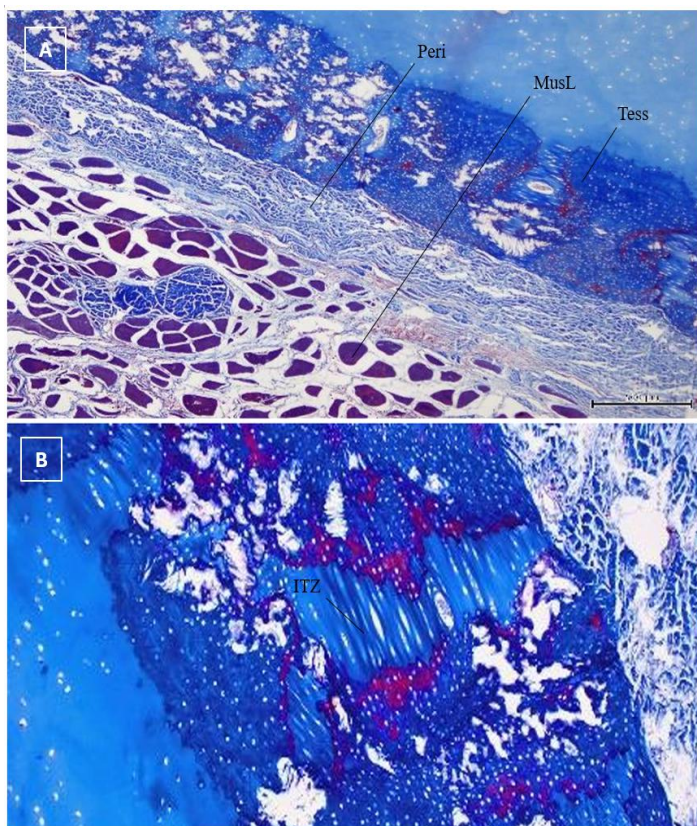


Figure 27. A: The MT staining illustrates the normal structure of healthy cartilage. The muscle layer is highlighted in red, while the perichondrium and the mineralized tesserae layer are depicted in deep blue. A detailed examination of the inter-tesserae fibrous zone (ITZ) shows blue staining from Masson's Trichrome (MT) and red delineation of tesserae fragments, indicating different types and maturation levels of collagen fibers. Abbreviation: ITZ – intertesserae fibrous zone; MusL – muscle layer; Peri – perichondral region; Tess – tesserae layers.





5.4 Description of the histopathology features of the skeleton lesions of the Butterfly ray (*Gymnura altavela*).

Upon the comprehensive elucidation of the normal histological architecture of the cartilaginous skeleton in *Gymnura altavela*, the histopathology of the traumatic lesion observed in the specimen (SA171-23) is subsequently analyzed. The traumatic impact on the scapulocoracoid joint elicited significant disorganization of its structural integrity, notably affecting the chain of the tesserae. As depicted in (Figure 28), these mineralized elements exhibit a pronounced separation from the non-mineralized core, mirroring the alterations observed in the adjacent perichondrium. This disjunction underscores the pathological changes induced by the trauma.

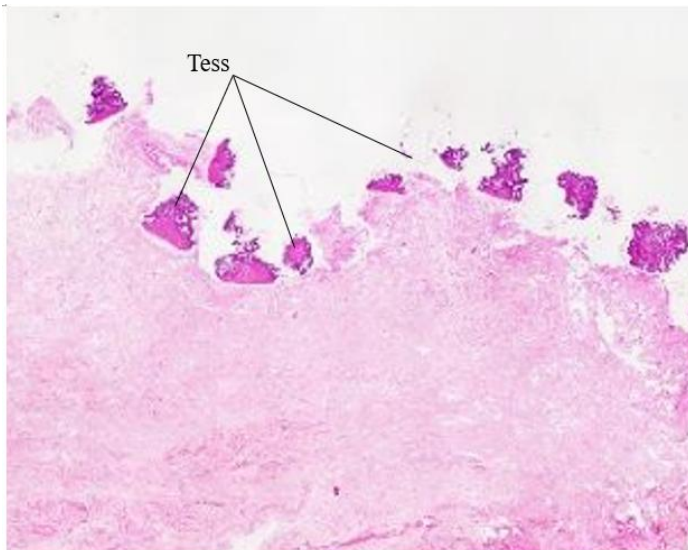


Figure 28. Histopathological examination of a synarcual-scapulocoracoid joint traumatized of the *Gymnura altavela* (SA171-23). The lesion is characterized by a loss of structural integrity in the tesserae layer and fractured pieces embedded within an abundance of fibrous tissue (H&E). Abbreviation: Tess – tesserae layers.

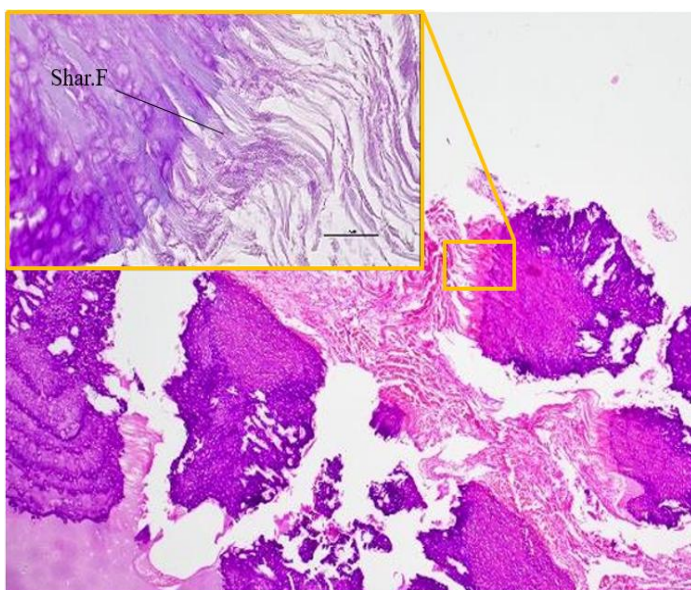


Figure 29. Histopathological examination of a synarcual-scapulocoracoid joint traumatized of the skeleton of the *Gymnura altavela* (SA171-23). A fractured and displaced piece of tesserae is evident (H&E), and the inset reveals frayed Sharpey's fibers (PAS). Abbreviation: Shar.F – Sharpey's fibers





Upon examining the tesserae at higher magnifications, it became increasingly evident that Sharpey's fibers, which play a crucial role in anchoring the perichondrium to the non-mineralized core, had experienced significant fragmentation and fraying. This deterioration has ultimately led to the rupture and damage of the perichondrium itself, as illustrated in (Figure 29). When assessing the lesion in its entirety, one can observe a pronounced disorganization and notable loss of the normal stratification that should typically characterize the various tissues surrounding the joint. For instance, there are considerable areas where the expected presence of articular muscle has been supplanted by abundant fibrous tissue, indicating that the muscle has been effectively replaced. This replacement suggests a disruption of normal physiological processes in the joint area. Moreover, the regions surrounding this fibrous tissue are densely populated with inflammatory cells, primarily granulocytes and mononuclear cells (Figure 30. A; B). These inflammatory cells indicate an active response to injury or irritation, further complicating the overall pathological landscape of the joint. This combination of structural alteration and inflammatory response underlines the severity of the lesion and its impact on joint functionality.

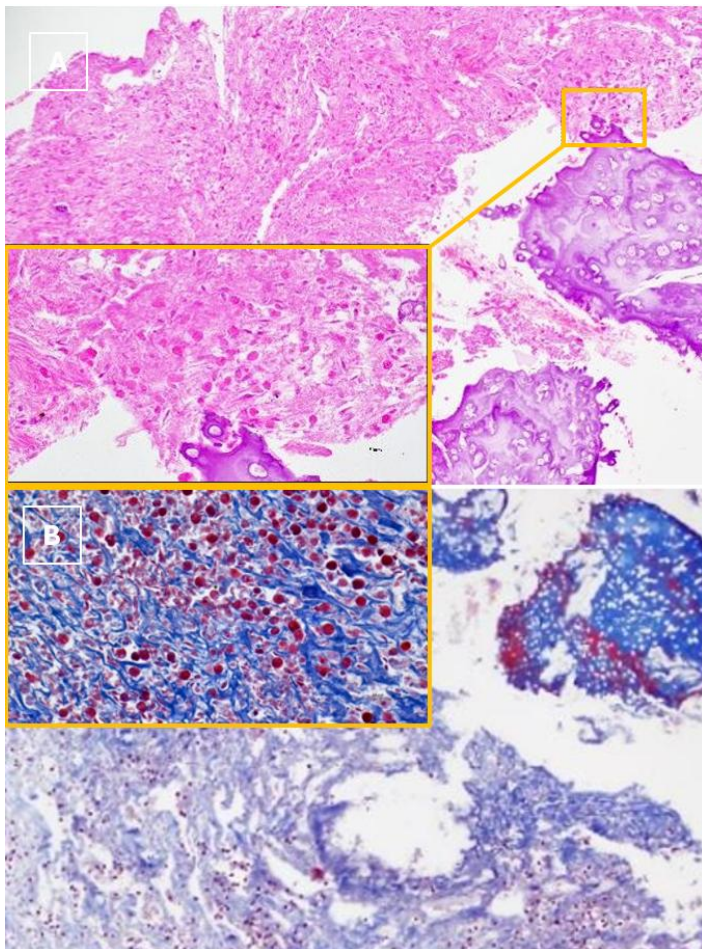


Figure 30. Histopathological examination of a synarcual-scapulocoracoid joint traumatized of the skeleton of the *Gymnura altavela* (SA171-23). A: There is a dense infiltration of inflammatory cells within the fibrous tissue (H&E). B: The absence of the muscular layer is confirmed, with granulocytes identified as the predominant inflammatory cells, as demonstrated by MT.





DISCUSSION

The elasmobranch group, including the spiny Butterfly ray, faces significant threats from direct human activities, such as overfishing, bycatch, and illegal trade, as well as indirect factors like habitat destruction and climate change. Together, these elements create a perfect storm, placing elasmobranchs—alongside sharks—among the most endangered species in the oceans. The extensive anthropogenic impact leads to numerous interactions between these species and humans, resulting in a variety of injuries and health issues, including hypoxia and trauma. Such injuries can range from wounds inflicted by hooks in the oral cavity, digestive tract, and gills, to penetrating and blunt-force trauma.

This investigation delineates a case involving a spiny butterfly ray (*Gymnura altavela*) that incurred a traumatic injury to the scapulocoracoid and synarcual cartilage. The etiology of this injury is attributed to an interaction with a penetrating and cutting fishing implement, presumably a spear, harpoon, or an analogous tool. This case underscores the potential impacts of anthropogenic activities on elasmobranch morphology and health. The injury was assessed through diagnostic imaging techniques like CT scans, which facilitated precise mapping of the affected region. The resulting incised-contused wound was situated dorsally on the right scapulocoracoid cartilage, resulting in considerable movement restrictions and subsequent deterioration of the specimen. The injury was characterized by significant disorganization of the mineralized cartilage, specifically referred to as tesserae. This condition was accompanied by a substantial presence of fibrous tissue and inflammation, with a high percentage of granulocytes. These findings suggest the occurrence of a chronic pathological process that severely compromised the animal's mobility. The application of imaging diagnostic modalities such as computed tomography (CT) scan post-mortem was performed to procure more intricate details regarding the injury, thus facilitating a more precise and thorough evaluation of the structural damage. This advanced imaging technique elucidated the lysis of the right scapulocoracoid cartilage, adversely affecting the articular surfaces that mediate the connection of the pectoral arch between the synarcual and scapulocoracoid cartilages.

Elasmobranchs, a subgroup within the class Chondrichthyes, are distinguished by their unique skeletal structure, which is entirely composed of cartilaginous tissue. This cartilaginous framework consists of multiple layers exhibiting varying degrees of mineralization, with the most highly mineralized layer referred to as tesserae, encompassing a core of unmineralized





cartilage. Surrounding this arrangement is the perichondrium, which nourishes and supports both the mineralized and unmineralized components. Cartilage is recognized for its avascular and aneural characteristics, significantly hindering its regenerative capabilities. This raises pertinent questions regarding the mechanisms of cartilage regeneration in elasmobranchs. In recent decades, there has been a divergence of opinions within the literature on this subject. Some studies, such as those by Ashhurst (2004), suggest a limited capacity for the recovery of the cartilaginous skeleton. Conversely, research by Seidel et al. (2017) indicates the potential for the development of cartilage-like tissue. Further contributions, notably by Marconi et al. (2020), have explored the presence of cartilage progenitor cells and the processes of chondrogenesis occurring in adult elasmobranchs. This ongoing discourse highlights the complexity of cartilage regeneration mechanisms and the need for further investigation to elucidate the extent of regenerative capabilities within this remarkable group of animals.

In the article "The Cartilaginous Skeleton of an Elasmobranch Fish Does Not Heal," published by Ashhurst in 2004, the question is posed: Did a mechanism for cartilage repair evolve in animals with cartilaginous skeletons? Through an experiment that lasted approximately 26 weeks, cuts were made in the fins of dogfish sharks, leading to an initial inflammatory response, followed by the development of fibrous tissue and subsequently cartilage-like tissue. However, this newly formed tissue was poorly vascularized and did not integrate with the existing cartilaginous tissue. As a result, Ashhurst concluded that Chondrichthyes cannot regenerate their cartilaginous skeleton. Thirteen years later, Seidel et al. published the article "Ultrastructural, Material and Crystallographic Description of Endophytic Masses: A Possible Damage Response in Shark and Ray Tessellated Calcified Cartilage" in 2017. This study described endophytic masses (EPM), which represent an aberrant development of mineralized cartilage-like tissue. Initially thought to be a form of cartilage repair, it was later determined that these masses exhibited distinct ultrastructural and chemical characteristics compared to tesserae, leading to the conclusion that their formation was likely due to a local breakdown in the processes that inhibit Ca P mineralization. Finally, the article "Adult Chondrogenesis and Spontaneous Cartilage Repair in the Skate, *Leucoraja erinacea*," published by Marconi et al. in 2020, reports for the first time the presence of cartilage progenitor cells and chondrogenesis in adult little skates. This study demonstrates their ability to spontaneously repair damaged cartilage, a process noteworthy for producing repair tissue that shares certain characteristics with normal cartilage and integrates seamlessly with the surrounding tissue.





The comprehensive description of the findings related to diagnostic imaging, along with the macroscopic and histological characteristics observed in the complete anatomopathological analysis conducted in this work, significantly enhances our understanding of the histopathological structure of this cartilage tissue following trauma. The study reveals a chronic lesion characterized by the disintegration of tesserae and a pronounced inflammatory response, indicating that the severity of the trauma has rendered tissue regeneration impossible. Overall, there remains a notable lack of detailed descriptions regarding the pathologies and traumatic injuries encountered in elasmobranchs.

CONCLUSIONS

1. The application of Computed Tomography (CT) has demonstrated significant value and reliability as a method for postmortem analysis of the macroscopic characteristics of anatomical structures in elasmobranch species. In the present study, this imaging technique facilitated a comprehensive visualization of the skeletal morphology in *Gymnura altavela*, highlighting its utility in advancing our understanding of the species' anatomical integrity.
2. The necropsy protocol utilized for the examination of the skeletal anatomy of elasmobranchs enabled systematic sampling for the analysis of the microscopic characteristics of the cartilaginous skeleton in the butterfly ray. This approach ensures a comprehensive understanding of the structural and functional aspects inherent to this group's unique skeletal composition.
3. Decalcification process was essential for the preparation of the skeleton samples to conduct its histological examination. The microscopic examination illustrates the structural components of healthy cartilage in *Gymnura altavela*. Noteworthy structures identified include the tesserae chain encircling the non-mineralized cartilage core, as well as Sharpey's fibers, which are integral to the overall composition and function of the cartilage.
4. The utilization of veterinary pathological anatomy, in conjunction with the descriptive methodologies it offers, has emerged as an indispensable resource for the comparative analysis and identification of pathologies associated with the skeletal structure of the species in question.
5. Advancements in tools such as CT imaging have facilitated the creation of detailed 3D representations of the cartilaginous skeleton of this species, enabling a thorough





examination of the trauma sustained by the specimen (SA171-23). This development has set a precedent for the anatomical description of the scapular girdle in *Gymnura altavela*.

6. Histopathology has been instrumental in this research, uncovering considerable degradation of the tesserae architecture within the scapulocoracoid cartilage. This degradation is marked by the detachment of tesserae from the underlying cartilaginous core. While some tesserae remain connected to the perichondrium through Sharpey's fibers, there was no indication of any regenerative processes occurring.

This study emphasizes the considerable lack of information regarding elasmobranchs. Through this research, the authors intend to close the knowledge gap surrounding this group of fish, which is increasingly affected by human-induced threats. This work aims to improve our understanding and management of elasmobranch populations amid escalating environmental pressures.

Part of this work has been recently published in the journal *Frontiers of Veterinary Sciences*, Montero-Hernández G, Caballero MJ, Curros-Moreno Á, Suárez-Santana CM, Rivero MA, Caballero-Hernández L, Encinoso M, Fernández A and Castro-Alonso A (2024) Pathological study of a traumatic anthropogenic injury in the skeleton of a spiny butterfly ray (*Gymnura altavela*). *Front. Vet. Sci.* 11:1452659. doi: 10.3389/fvets.2024.1452659





BIBLIOGRAPHY

F. Serena, A. J. Abella, F. Bargnesi, M. Barone, F. Colloca, F. Ferretti, F. Fiorentino, J. Jenrette & S. Moro (2020) Species diversity, taxonomy and distribution of Chondrichthyes in the Mediterranean and Black Sea, *The European Zoological Journal*, 87:1, 497-536, DOI: 10.1080/24750263.2020.1805518

Fisheries and Oceans Canada. (s.f.). Internal anatomy of skates. Recuperado de <https://www.dfo-mpo.gc.ca/species-especies/skates/anatomy/internal-eng.html>

Food and Agriculture Organization. (2006). Field identification guide to the sharks and rays of the Mediterranean and Black Sea. Food & Agriculture Organization of the United Nations (FAO).

Gárquez Ortiz, A., Plana, M. Á. S., & Blanco-Morales, Á. T. R. (1989). La necropsia en los mamíferos domésticos. Madrid. Interamericana: McGraw-Hill, 1989.

Geraci, M.L.; Ragonese, S.; Scannella, D.; Falsone, F.; Gancitano, V.; Mifsud, J.; Gambin, M.; Said, A.; Vitale, S. Batoid Abundances, Spatial Distribution, and Life History Traits in the Strait of Sicily (Central Mediterranean Sea): Bridging a Knowledge Gap through Three Decades of Survey. *Animals* 2021, 11, 2189.

González Pajuelo, José M. Taxonomía, morfología, anatomía y muestreo biológico de Elasmobranquios. Universidad de Las Palmas de Gran Canaria, Departamento de Biología, Métodos en Investigación Pesquera.

Hall, K. C., Hundt, P. J., Swenson, J., Summers, A., & Crow, K. D. (2018). The evolution of underwater flight: The redistribution of pectoral fin rays, in manta rays and their relatives (Myliobatidae). *Journal of Morphology*. DOI: 10.1002/jmor.20837.

Huang, W., Hongjamrassilp, W., Jung, J.-Y., Hastings, P. A., Lubarda, V. A., & McKittrick, J. (2017). Structure and mechanical implications of the pectoral fin skeleton in the Longnose Skate (Chondrichthyes, Batoidea). *Acta Biomaterialia*, 51, 393-407. <https://doi.org/10.1016/j.actbio.2017.01.026>

INVEMAR. (s.f.). Componente tiburones, rayas y quimeras en Colombia. SiAM. Recuperado de <https://tiburones.invemar.org.co/>





- Johanson, Z., Martin, K., Fraser, G., & James, K. (2019). The synarcual of the little skate, *Leucoraja erinacea*: Novel development among the vertebrates. *Frontiers in Ecology and Evolution*, 7, 12. <https://doi.org/10.3389/fevo.2019.00012>
- Kobelkowsky, A. (2017). Anatomía comparada del neurocráneo y el encéfalo de la raya mariposa *Gymnura micrura* (Batoidea: Gymnuridae). *International Journal of Morphology*, 35(2), 644-650.
- Last, P., Naylor, G., Seret, B., White, W., Stehmann, M., & de Carvalho, M. (Eds.). (2016). *Rays of the world*. CSIRO Publishing
- Long, D. and Walford, Lionel A. (2024, October 4). chondrichthyan. *Encyclopedia Britannica*. <https://www.britannica.com/animal/chondrichthian>
- Marconi A, Hancock-Ronemus A, Gillis JA. Adult chondrogenesis and spontaneous cartilage repair in the skate, *Leucoraja erinacea*. *eLife*. (2020) 9:e53414. Doi: 10.7554/eLife.53414
- Montero-Hernández, G., Caballero, M. J., Curros-Moreno, Á., Suárez-Santana, C. M., Rivero, M. A., Caballero-Hernández, L., Encinoso, M., Fernández, A., & Castro-Alonso, A. (2024). Pathological study of a traumatic anthropogenic injury in the skeleton of a spiny butterfly ray (*Gymnura altavela*). *Frontiers in Veterinary Science*, 11, 1452659. <https://doi.org/10.3389/fvets.2024.1452659>
- Navia, A. F., & Mejía-Falla, P. A. (2011). *Guía para la identificación de especies de tiburones y rayas comercializadas en el Pacífico colombiano*. Fundación SQUALUS y Conservación Internacional Colombia.
- Nishida, K. (1990). Phylogeny of the suborder Myliobatidoidei. *Memoirs of the Faculty of Fisheries Hokkaido University*, 37(1-2), 1-108. <https://hdl.handle.net/2115/21887>
- Parsons, K. T., Maisano, J., Gregg, J., Cotton, C. F., & Latour, R. J. (2018). Age and growth assessment of western North Atlantic spiny butterfly ray *Gymnura altavela* (L. 1758) using computed tomography of vertebral centra. *Environmental Biology of Fishes*, 101(1), 137–151. <https://doi.org/10.1007/s10641-017-0687-x>
- Seidel R, Blumer M, Zaslansky P, Knötel D, Huber DR, Weaver JC, et al. Ultrastructural, material and crystallographic description of endophytic masses—A possible damage response





in shark and ray tessellated calcified cartilage. *J Struct Biolo* (2017) 198:5–18. doi: 10.1016/j.jsb.2017.03.004

Adams, K. R., Fetterplace, L. C., Davis, A. R., Taylor, M. D., & Knott, N. A. (2018). Sharks, rays, and abortion: The prevalence of capture-induced parturition in elasmobranchs. *Biological Conservation*, 217, 11–27. <https://doi.org/10.1016/j.biocon.2017.10.010>

Amaral, C. R., Pereira, F., Silva, D. A., Amorim, A., & de Carvalho, E. F. (2018). The mitogenomic phylogeny of the Elasmobranchii (Chondrichthyes). *Mitochondrial DNA Part A*, 29, 867–878.

Ashhurst, D. E. (2004). The cartilaginous skeleton of an elasmobranch fish does not heal. *Matrix Biology*, 23(1), 15-22. <https://doi.org/10.1016/j.matbio.2004.02.001>

Bonfil, R., & Abdallah, M. (2004). Field identification guide to the sharks and rays of the Red Sea and Gulf of Aden. *FAO Species Identification Guide for Fishery Purposes*. Food and Agriculture Organization of the United Nations (FAO).

Carrier, J. C., Musick, J. A., & Heithaus, M. R. (Eds.). (2012). *Biology of sharks and their relatives* (2a ed.). CRC Press.

Claeson, K. M. (2008). Variation of the synarcual in the California Ray, *Raja inornata* (Elasmobranchii: Rajidae). *Acta Geologica Polonica*, 58(2), 121-126.

Compagno, L. J. V. (1999). Endoskeleton, in *Sharks, Skates, and Rays: The Biology of Elasmobranch Fishes* (C. Hamlett, Ed.). Johns Hopkins University Press.

Compagno, L. J. V. (2005). Checklist of Chondrichthyes. In W. C. Hamlett (Ed.), *Reproductive Biology and Phylogeny of Chondrichthyes: Sharks, Batoids, and Chimaeras* (pp. 503–547).

Cousseau, M. B., Figueroa, D. E., Díaz de Astarloa, J. M., Mabragaña, E., & Lucifora, L. O. (2007). Rayas, chuchos y otros batoideos del Atlántico sudoccidental (34° S-55° S). Instituto Nacional de Investigación y Desarrollo Pesquero (INIDEP).

Dulvy, N. K., Charvet, P., Carlson, J., Badji, L., Blanco-Parra, M. P., Chartrain, E., & others. (2021). *Gymnura altavela*. The IUCN Red List of Threatened Species 2021: e.T63153A3123409. <https://doi.org/10.2305/IUCN.UK.2021-1.RLTS.T63153A3123409.en>





Ebert, D. A., & Stehmann, M. F. W. (2013). Sharks, batoids, and chimeras of the North Atlantic (FAO Species Catalogue for Fishery Purposes No. 7). Food and Agriculture Organization of the United Nations (FAO).

Espino-Ruano, A., Castro, J. J., Guerra-Marrero, A., Couce-Montero, L., Meyers, E. K. M., Santana-del-Pino, A., & Jiménez-Alvarado, D. (2023). Aggregative behavior of spiny butterfly rays (*Gymnura altavela*, Linnaeus, 1758) in the shallow coastal zones of Gran Canaria in the Eastern Central Atlantic. *Animals*, 13(1455). <https://doi.org/10.3390/ani13091455>

